Proportional-Derivative-Acceleration Feedback Controller Design For Single Axis Attitude Control Of Rigid Spacecraft With Flexible Appendages

Anirudh Agarwal

A thesis submitted to the Faculty of Graduate Studies

in partial fulfilment of the requirements for the degree of

Master of Science

Graduate Program in Earth and Space Science

York University

Toronto, Ontario

November 2018

Abstract

This study designs and analyzes a new type of controller that helps improve the performance of single axis attitude control of flexible appendages attached to a rigid spacecraft. Conventionally, PID with position feedback was used to control single axis attitude manoeuvre of flexible appendages on a spacecraft but designing a PID to control a higher order system is a limited strategy. Also, PID controllers are inherently unstable for third order systems and higher as will be demonstrated later. Thus, acceleration feedback is included in the design to demonstrate a more stable way of designing controllers for these systems and it is called PDA (Proportional Derivative Acceleration) controller. The controller is first designed using a root locus method and then applied to a simulated third order system om MATLAB. Then a higher order system model (rigid body with flexible appendage) is created on SIMULINK and the controller is applied to it. Finally, an experiment is performed and demonstrated to show the practical implementation of the control design.

Acknowledgement

I would like to thank the late Professor George Vukovich for guiding me through my master's education and helping me develop the core of my thesis. He was a great mentor and a teacher. He taught me control systems and Finite element methods in my undergraduate studies which ultimately help shape my research interests. He also helped me write my first journal paper and was supportive of any research interest that I brought up.

I would also like to thank Professor Zheng Hong Zhu for taking over my research after Professor Vukovich's passing. He helped me write my thesis and compile all my thoughts in a coherent form. I also thank him for including me as a part of his research team and providing me opportunities in the field of attitude control, so I continue my research interests beyond my Masters.

Table of Contents

List of Figures

Symbols and Conventions

All unites are given in SI units, time in seconds (s), distance in metres (m), angular rotation in radians per seconds, velocity in metres per second and frequency in Hertz.

All vectors are shown in bold letters in the equations and all the matrices have a square bracket surrounding them. All Greek letters are italic to not confuse them with English letters. All scalars are denoted as regular font (not bold).

List of symbols

a	real pole of the PDA controller
$\mathbf{h_B}$	Angular momentum vector of rigid body
e(t)	error between desired value and measured value
I	Inertia matrix of rigid body
I_e	Inertance (quantity defined in Eq. 5-8)
I_f	Inertia of flexible body
k_p	Proportional gain
k_d	Derivative gain
k_a	Acceleration gain
k_i	Integral gain
q	Generalized coordinates for representing flexibility
r	Position vector of an infinitesimal mass dm on the flexible appendage .
Z	Damping coefficient of flexible mode
δ	Deformation of flexible body.
σ	Density distribution of the flexible body.
T	Torque on rigid body
u	Control torque vector
z_1	first zero in the PDA controller
z_2	second zero in the PDA controller
$\boldsymbol{\omega_B}$	Angular velocity vector of rigid body
θ	Angle vector of rigid body

ω_a Pole of the actuator used to drive the rigid body.

ω_s Pole of the sensor used to measure angle of the rigid body.

ω_{cp} Phase crossover frequency

Ω Natural frequency of the flexible modes

ξ damping ratio of complex pole system

ω natural frequency of complex pole.

List of Abbreviations

PDA Proportional-derivative-acceleration

PID Proportional-integral-derivative

PIDA Proportional-integral-derivative-acceleration

SISO Single input single output

PIID Proportional-integral-integral-derivative

MEMS Micro-Electro-Mechanical-Systems

FOPDT First order Plus Delay Time

ISS International Space Station

AVR Automatic Voltage Regulator

CTS Communications Technology Satellite

Chapter 1 INTRODUCTION AND JUSTIFICATION

Summary: In this chapter, we define the problem, justify undertaking the research and provide the objectives that we set out to achieve. Furthermore, we provide our research methodology and a summary of the layout of the thesis.

1.1 Flexible Spacecraft

Large flexible space structures have been in and out of vogue over the past few decades, with the most ambitious being the proposed large solar power satellites of the 1980's. Solar sails and non-furlable antennas are flexible structures that could be considered extreme cases of flexibility whose realizable technology is still far off. Typical examples of flexible spacecraft are rigid bodies with elastic appendages such as large antennas, which still possess a reasonable amount of flexural rigidity. It is this type of system to which we direct our attention below. In [1,2,3], the flexibility of the communications technology satellite CTS spacecraft is studied at length. These spacecrafts are characterized by their lightly damped vibrations, limited number of sensors and actuators for control and the fact that the model of these spacecraft may not be fully realized before they are deployed. One of the more famous models of a flexible appendage is the CANADARM [4]. Thus, it is imperative that we develop better control mechanisms to stabilize these spacecrafts.

To date, there has been an immense number of researches on modelling and control design for flexible space structures, much of it based on the sophisticated methods of modern control theory. However, for certain circumstances classical methods are perfectly adequate. In the classical sense, a rigid spacecraft can be considered a second order system and any subsequent actuators and sensors attached to it increase the system order to a third or a fourth order system. When we consider the addition of flexible appendage(s) to this system, our model now increases drastically from a third order to an nth order system where n is a large number, for example 20. In [2,3] the CTS spacecraft was approximated to have 12 modes and thus would be a 26^{th} order system at minimum (2 rigid body poles + 24 flexible body poles). Thus, in our work we consider tackling the higher order model and develop controllers for them. We are providing a methodology to control only a single axis of the spacecraft and this assumption is described in detail in Section 2.

Several methods have been used in the past to, among other things, design Proportional-integral-derivative (PID) controllers for rigid body spacecraft and evaluate their stability and performance when flexible appendages are subsequently attached to the rigid bodies [1, 2]. In this work controllers for the same type of spacecraft, i.e. rigid hub with flexible appendages, are developed to improve the stability and the transient response of the attitude control system of these spacecrafts by designing for the flexible appendages directly instead of for the rigid body. This is done by introducing acceleration feedback to a proportional-derivative feedback controller. A tuning procedure for the control of higher order systems using PDA (Proportional-Derivative-Acceleration) controllers using the root locus method is proposed.

1.2 Limitation of Existing Research

In this section, we elaborate on why using a simple PID on position feedback can lead to instability when trying to control position of rigid body spacecraft. We have already discussed how a rigid spacecraft at minimum can be modelled as a third order system. As shown in Figure 1-1, the root locus of a PID controller used to control a third order system. As the gain of the system is increased the poles could end up in the right half plane making the system unstable. This is because the closed loop system would have four poles and two zeros, thus not all the poles decays into their respective zeros.

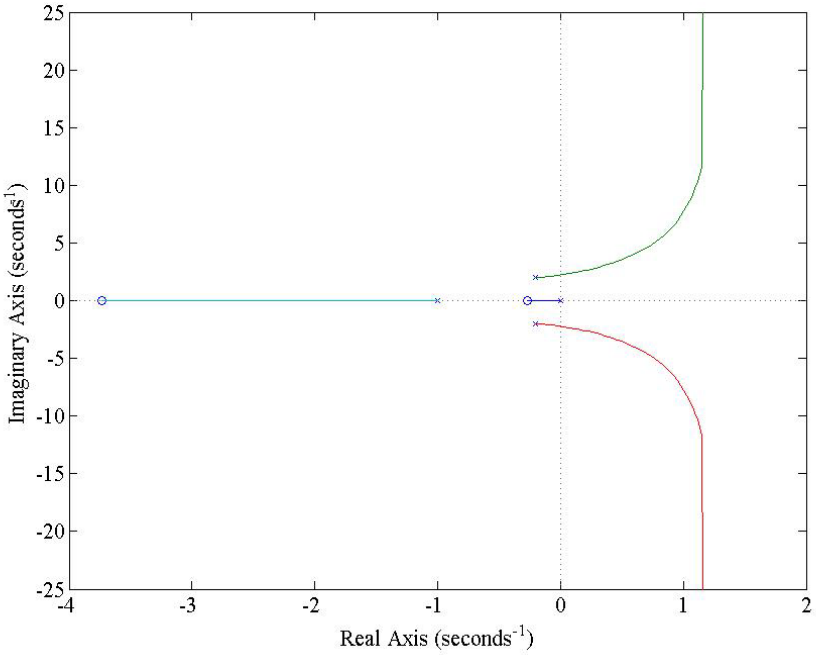

Figure 1-1: Root Locus of PID controller for a third order system.

We can design the zeros in such a way that the poles do not enter the right half plane as well, but this means that system model must be more robust as uncertainties could make the system unstable without intention. In [1] and [2], the authors use a PID to place the poles of the rigid spacecraft in a pre-determined desired position, but they are limited

by the fact that the characteristic polynomial of their system has 4 desired coefficients and only three control parameters i.e. proportional, derivative and acceleration feedback gains. They circumvent the problem by fixing the real axis coefficients of their desired poles and vary the imaginary axis to reduce the number of undetermined coefficients. Both these limitations can be solved be simply introducing adding an acceleration feedback term [5] in the controller as in Figure 1-2.

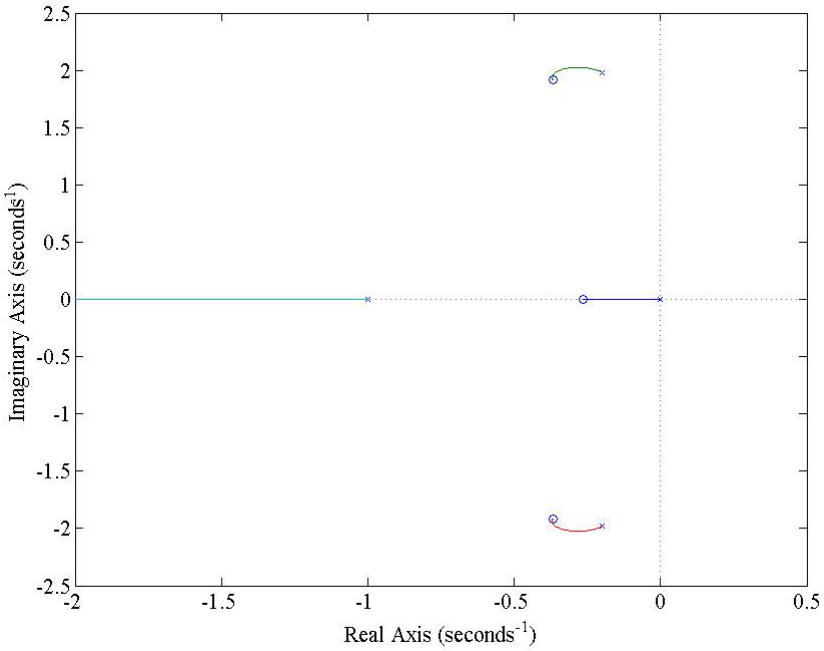

Figure 1-2: Root Locus of PIDA controller for a third order system.

As can be seen in the Figure 1-2, the system has 4 poles and 3 zeros thus we not only have better control of the system, we also improve the stability of the system. Thus from [5] and verifying from our own analysis we can see that PID with position feedback is inherently unstable for a third order system while adding the acceleration term stabilizes it.

Therefore, we focus our attention to the addition of acceleration feedback to control these higher order systems better. A more detailed literature review of acceleration

feedback in control systems is provided in section 2.5. In short, the limitations are the fact that the controllers are reliant on the exact model of the system which makes the system limited as any uncertainties would provide undesired effects on the system response [5, 6]. Differentiating a signal and adding it to the feedback of the system introduces a problem of causality as we need to know the future to know the rate of change of the system variable. To solve the problem, we introduce filters to the differentiating terms so that the system remains causal. The controllers in [5 and 6] do not address the problem of an optimal value of the addition of filters to render the system causal which we attempt to address alter.

1.3 Objectives of the Research

The objectives of this work are to:

(i) Evaluate whether addition of acceleration feedback will improve the response of third order systems. Evaluate the viability of the approach for higher order systems.

(ii) Develop a control algorithm to include acceleration feedback and simulate its response. Compare it with the results obtained with a conventional PID with position feedback.

(iii) Perform experiments with a higher order system (flexible link attached to a motor).

(iv) Apply the algorithm to the flexible spacecraft (CTS) and compare the results with the controllers that were used to slew the spacecraft.

1.4 Method of Research

The core of this research can be divided into three phases. The first phase is the theoretical phase where we identify the impact of adding acceleration feedback to third order systems and other higher order systems. Then we move on to developing the control algorithm to

try and control a third order system. We extend this framework for higher order systems theoretically and observe its impact. In the second phase we perform experiments with a flexible link to try and control the system using our algorithm. In the third phase we apply this control algorithm to try and control the slew response of the CTS spacecraft and observe if the output is better than the ones produced by PID controllers developed then.

1.5 Research Methodology

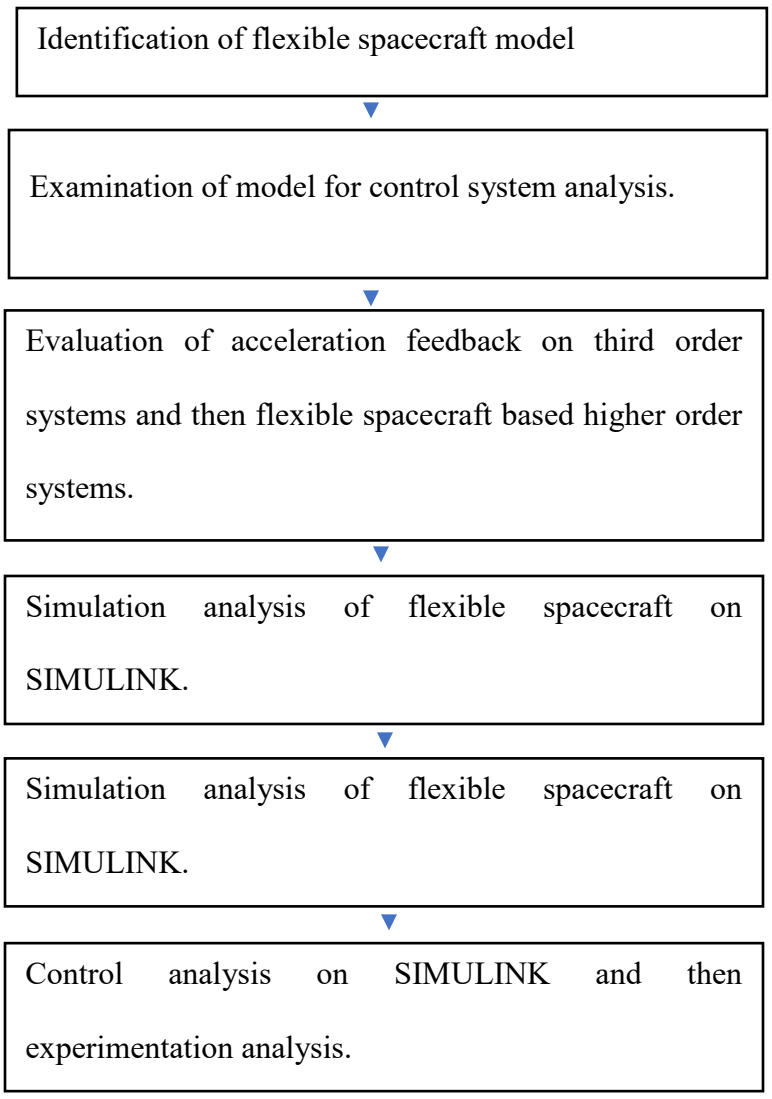

1.6 Layout of Thesis Document

This thesis contains 5 chapters. In Chapter 2 we provide a literature review of when acceleration feedback was utilized to control higher order systems and the limitations of the existing methods. In Chapter 3 we introduce our tuning mechanism that addresses the problems stated above. In Chapter 4 we show the results of using our controller in an experiment. In Chapter 5 we show how a flexible spacecraft can be controlled using our controller.

Chapter 2 LITERATURE REVIEW AND MOTIVATION

Summary: In this chapter we review some of the theory of dynamically modelling rigid and flexible spacecraft. We then provide a literature review on some existing control techniques that can be utilized to improve slewing response of these spacecraft. Finally, we provide motivation behind pursuing our research and a literature review on some of the techniques used in the field.

2.1 Rigid Body Spacecraft Control Problem Formulation

Consider a rigid spacecraft with three degrees of freedom as presented in Figure 1. The angular momentum in the body fixed coordinates is given by

$$\mathbf{h_B}=[\mathbf{I}]\boldsymbol{\omega}_\mathbf{B} \tag{2-1}$$

where $\mathbf{h_B}$ is the angular momentum vector and $\boldsymbol{\omega}_\mathbf{B}$ is the angular velocity vector, and $\mathbf{I}$ is the moment of inertia of the rigid body.

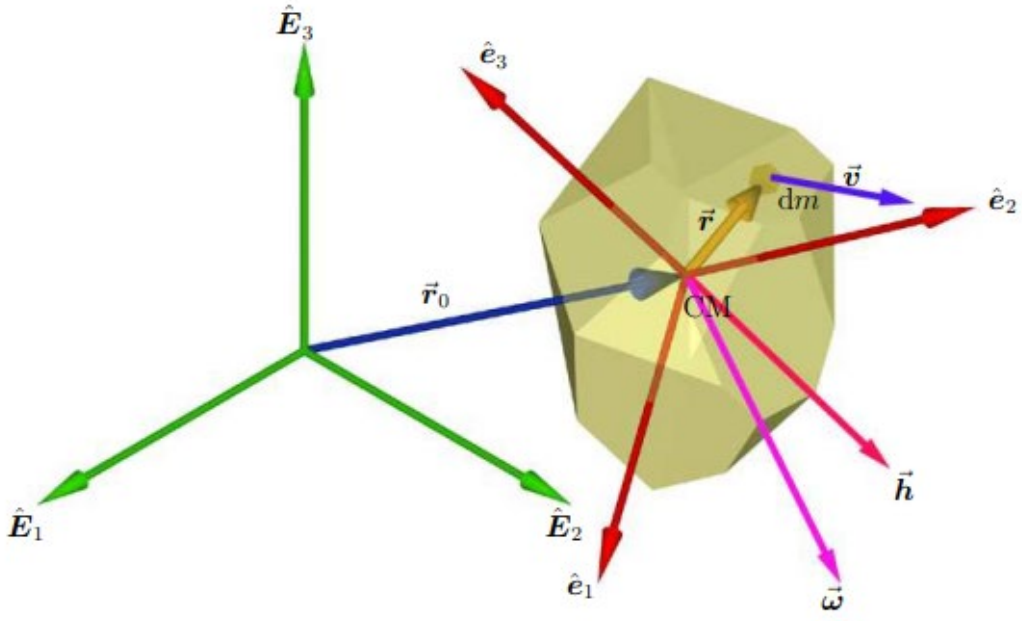

Figure 2-1: Inertial and body fixed coordinate systems for a rigid satellite.

Here the axes E_1, E_2 and E_3 are the axes of inertial frame, while e_1 ,e_2 and e_3 are in the body fixed frame. By applying the Euler's equation of motion, we can derive the dynamics of the rigid spacecraft. Assuming the inertia matrix is constant, we get

$$[\mathbf{I}]\dot{\boldsymbol{\omega}}_{\mathrm{B}}+\boldsymbol{\omega}_{\mathrm{B}}\times([\mathbf{I}]\boldsymbol{\omega}_{\mathrm{B}})=\mathbf{u} \tag{2-2}$$

where $\mathbf{u}$ is the torque that is applied to the body. If the rotation is slow, the angular velocity can be treated as a small perturbation of the steady state, such that $\| \boldsymbol{\omega}_{\mathrm{B}} \| \ll 1$. Thus, the cross-coupling term $\boldsymbol{\omega}_{\mathrm{B}}\times(\mathbf{I}\boldsymbol{\omega}_{\mathrm{B}})$ is negligible. Euler's equations then become

$$[\mathbf{I}]\dot{\boldsymbol{\omega}}_{B}=\mathbf{u} \tag{2-3}$$

In this work, we are only interested in solving the rotational dynamics about a single axis so that the system can be represented as a single input single output system. Accordingly, Eq. (2-3) is simplified for the dynamics of the single axis are

$$\mathrm{I}\ddot{\theta} = \mathrm{u}\,, \tag{2-4}$$

where here the I refer to the moment of inertia of the axis we are trying to model and control and θ is the angle about the rotational axes of the spacecraft.

Equation (2-4) can be transformed into the frequency domain by applying the Laplace transformation.

$$\frac{\theta(\mathrm{s})}{\mathrm{u}(\mathrm{s})}=\frac{1}{\mathrm{Is}^{2}}\,, \tag{2-5}$$

If we have the sensors required to feedback the current angle or angular velocity of the satellite, we can use that to provide feedback to the controller to provide a desired response as presented in Figure 2-2. Let us assume a general actuator providing the control

torque to the satellite. Examples of actuators could be jet thrusters, reaction wheels, control moment gyroscopes etc.

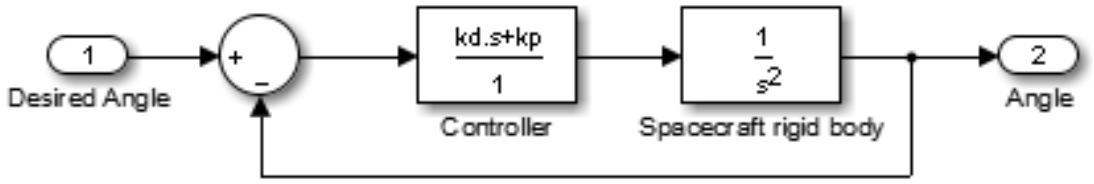

Figure 2-2: Proportional-derivative gain feedback block diagram for a rigid spacecraft.

Let $\theta_d(t)$ be the desired angle, the feedback controller thus becomes

$$u(t)=k_d\dot{e}(t)+k_p e(t), \tag{2-6}$$

where $e(t)=\theta_d(t)-\theta(t)$, $\dot{e}(t)=\dot{\theta}_d(t)-\dot{\theta}(t)$

The closed loop system in Figure 2-2 in the frequency domain becomes

$$\frac{\theta(s)}{\theta_d(t)}=\frac{(k_d s+k_p)}{(Is^2+k_d s+k_p)}, \tag{2-7}$$

Thus, the system has one zero and two poles. The solution to this second order differential equation is a decaying exponential. However, in practical terms, this controller may not work well, since it assumes that the actuator and sensors would provide perfect response. If we let the actuator have a first order dynamic response as in Figure 2-3, the open loop system becomes

$$\frac{\theta(s)}{u(s)}=\frac{s}{s^2(s+\omega_a)}, \tag{2-8}$$

This system is of a third order and we have shown above in Section 2.1 how using conventional PID control makes this system naturally unstable. Therefore, in the following

chapter we begin by addressing third order systems and use acceleration feedback to improve the response of the rigid spacecraft attitude control system.

2.2 Flexible Spacecraft Problem Formulation

Consider a flexible appendage attached to a rigid spacecraft as shown in Figure 2-3. It is assumed that the motion of one axis's attitude is uncoupled from the motion about the other two axes as we derived above in section 2.1 due to small angle maneuvers. We also assume Euler-Bernoulli deformation i.e. the deformation only occurs in the y-direction as specified in Figure 2-3. The equations of motion derived below are a first order approximation of the general model of elastic displacement of a flexible spacecraft. In Hughes's model it is also assumed that the significant frequency content of any disturbances (due to gravity gradient or other environmental effects) are on the lower end of controller band pass and will thus get rejected. The motion equations in the time domain [7 and 8] are

$$I\ddot{\theta} + \int_A \mathbf{r}^x \ddot{\boldsymbol{\delta}}(\mathbf{r},t)\boldsymbol{\sigma}(\mathbf{r})d\mathbf{v} = \mathbf{T}(t) \tag{2-9}$$

where **I** is the moment of inertia of the rigid body, **r** is the position of the infinitesimal mass dm in Figure 2-3, $\boldsymbol{\delta}(\mathbf{r})$ is the deformation of the flexible body, $\boldsymbol{\sigma}(\mathbf{r})$ is the density distribution of the flexible body and $T(t)$ is the torque applied to the body. Equation (2-9) is a generalized way of showing the effect of flexible appendages on the single axis attitude control of a spacecraft. We assume that the torque is applied to the rigid body, for example via reaction wheels or jet thrusters.

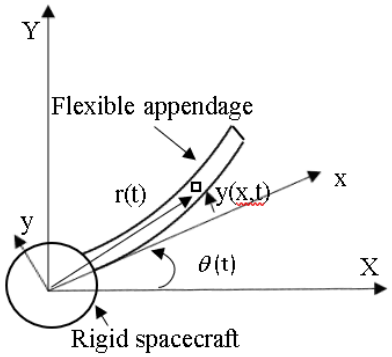

Figure 2-3: Free body diagram of flexible appendage attached to a rigid spacecraft.

There are several ways to convert Eq, (2-9) to a linear system which can be controlled. One of the ways is to assume that the resulting motion of the spacecraft is a superposition of natural modes of the system. The deformation is assumed to be sinusoidal ie.

$$\delta(r,t) = \sum_{n=1}^{N} q_n \cos(\Omega_n t) \tag{2-10}$$

where q_n is the nth modal coordinate that accommodates for the degrees of freedom of the flexible appendage, Ω_n is the natural frequency of the nth mode and N is the number of modes. Substituting Eq. (2-10) into (2-9) and then performing several algebraic operations (performed in [8]) we eventually get the time domain representation of the flexible spacecraft.

$$I\ddot{\theta}(t) + \sum_{n} h_n \ddot{q}_n(t) = T(t) \tag{2-11}$$

$$h_n \ddot{\theta}(t) + I_f(\ddot{q}_n(t) + 2Z_n\Omega_n \dot{q}_n(t) + \Omega_n^2 q_n(t)) = 0 \tag{2-12}$$

where q_n is a "modal coordinate" associated with n-th vibration mode of the appendages, $h_n q_n$ is the angular momentum of the system, Z_n is the damping ratio of the flexible mode, Ω_n is the natural frequency of the flexible mode and T(t) is the control torque

applied by the attitude control system. This method is popularly referred to as the **"assumed modes method"** [1]. As we can see in Eq. (2-11), it is an extension of Eq. (2-4). The force applied by the attitude control system influences the flexible modes present in the system. In the following sections we review the different control approaches in rigid body and flexible body spacecraft control. We only concern ourselves with a single axis control of flexible appendages since we have assumed small angle rotations so that we can minimize the coupling.

2.3 Rigid Body Controller Design Review

Consider a general third order system consisting of one real pole and two complex poles of the form:

$$\frac{Y(s)}{U(s)} = G(s) = \frac{K}{(s+a)(s^2 + 2\xi\omega_n s + \omega_n^2)} \tag{2-13}$$

where Y(s) is the output of the system, U(s) is the control input to the system, K is the gain acting on the system, the real root is -a, the damping ratio of the complex poles is ξ and the natural frequency is ω. We concern ourselves with a third order system because the open loop control system in Eq (2-8), which represents the model of a single axis attitude control system, was of third order.

There are several ways one can control a third or higher order system using a PID. One way is to reduce a higher order system to a second order or first order system and control the reduced order model instead. In [9], a higher order system was reduced to a FOPDT [First Order Plus Delay Time] system and then a PID control law was derived by using a tuning procedure via a maximum sensitivity function. In [10] a higher-order oscillatory system was first reduced to a reduced third order system with time delay, and

then a PID control law is derived to produce their desired response. Even though PID controllers are used to control a third order system, we have shown in Section 1.2 that PID is inherently unstable for a third order system.

In [11] the authors simplified the attitude control system derivation such that they control the roll and yaw motion of the spacecraft by placing the poles in a desired location via simple negative feedback gain. In [12] the authors simply design a lead-lag controller to place the poles in such a way that it yields a 50 percent damped system. Another set of methods in designing a controller is in [13] where the authors design a controller based on an optimal reaction wheel power criterion where a certain condition is first applied and then the control law is derived such that it satisfies that condition. In [14] the author implements a simple PD control to control a single axis of a satellite using a reaction wheel, but provides a comprehensive study on how it is affected by different disturbances like sinusoidal, impulse etc. In [1] and [2] the authors provide a methodology to place the rigid body poles using PID, which will essentially form the basis for our research.

2.4 Flexible Appendages Control Review

In Figure 4, we show how to model a single axis attitude control of rigid hub with a flexible appendage attached to it from Ref. 1. In [1], the author designs a PID control for the rigid part of the spacecraft and then analyses under what conditions would incorporating the flexible modes destabilize the system. In [2] the authors use the same model and procedure from Ref 1 but use a different way of generating gain values for PID and PIID controllers.

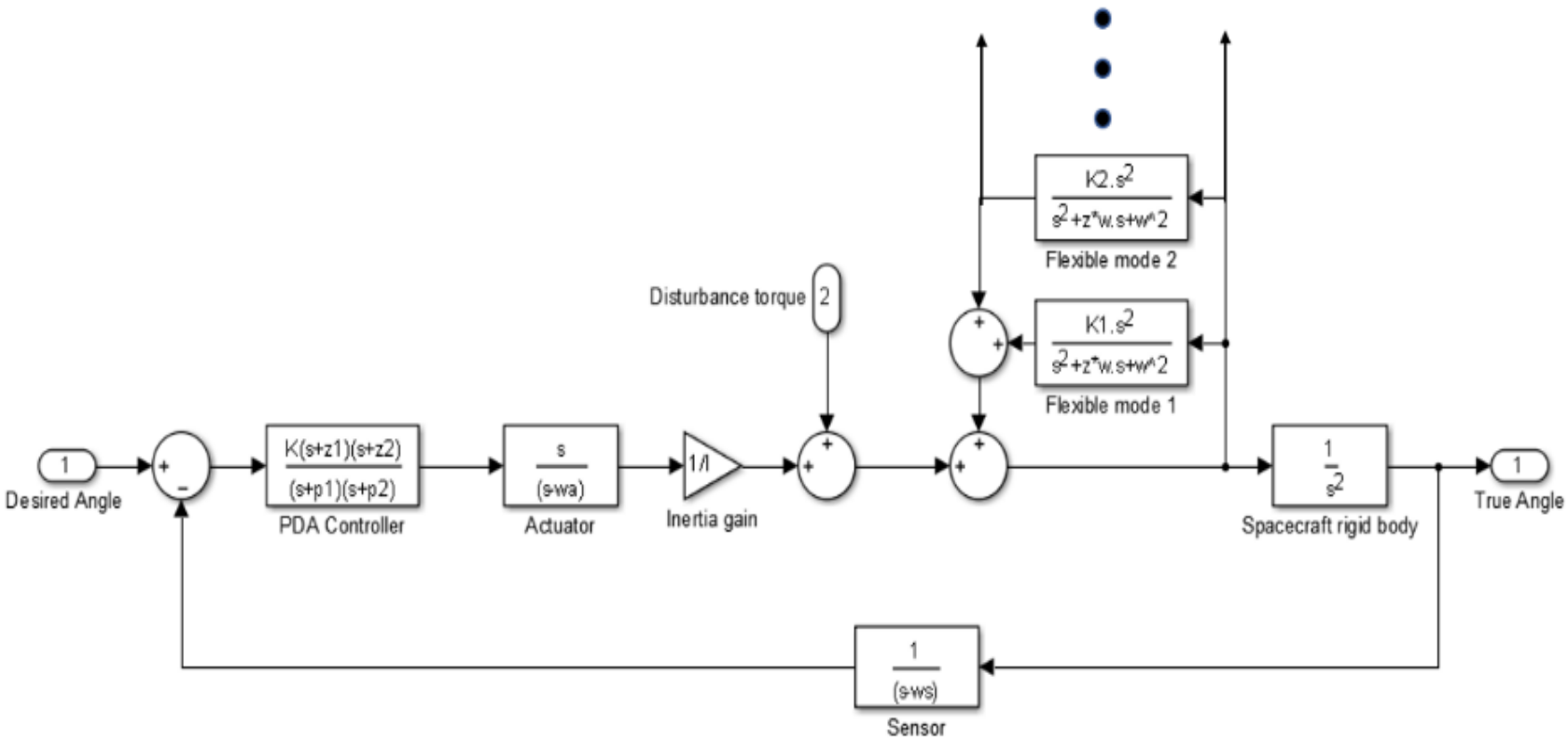

Figure 2-4: Single axis control of rigid body spacecraft attached to flexible appendages with n flexible modes block diagram [1].

In [15], the authors design a single axis attitude control system for rotational manoeuvres of flexible spacecraft using optimal control theory. In [16], the author designs a popular approach to control rest to rest manoeuvres of flexible spacecraft using passivity principles. It basically proves that the transfer function between the control input and angular velocity is passive, and thus providing any strictly positive feedback would stabilize the system asymptotically.

In [17], the author designs a an on-off thruster type control to control a flexible appendage attached to a rigid body. In the paper it is also shown that if the gain values are above a certain value, it makes the system unstable and lowering the gain values reduces the performance of the system. In [18] a non-minimum phase filter has been designed to control the system. In [19] the authors use a disturbance rejection control approach to use control moment gyros to stabilize the ISS.

In literature we find that the small deformation approximation used in section 2.1 and 2.2 does not work very well for large angle manoeuvres. If a Timoshenko beam model is used instead of Euler Bernoulli model, then we can consider larger deformations. In general, for a three-axis satellite with flexible appendages if angular velocity feedback is present, passivity-based control design [16, 33, 34] provide a robust way to ensure asymptotic stability. In [20] the authors develop an optimal control problem using linear quadratic regulator to provide three axis stabilization of a flexible spacecraft. The literature that we provided is mostly concerned with classical approaches since they are intuitive and there is a lot of work done with SISO systems and frequency domain controllers. In [23] the authors show an active robust shape control procedure to control flexible structures. In

[24] the authors have provided a zero-residual-energy approach using bang-bang control to perform single axis slewing of flexible spacecraft. In [33] the authors provide a positive position feedback control for large space structures. In [34] the authors develop a direct velocity feedback control of large space structures. In [35] the authors present a passivity-based attitude control with input quantization. In [36] the author presents a passivity-based control design with non-collocated sensors and actuators.

2.5 Motivation for Research

We mentioned in Section 2.1 that the authors in references [1] and [2] provided a technique to place the poles of the system using PID to a desired location and used that to control the rigid body of the spacecraft. They then add the flexible modes to the system later and verify whether it makes the system unstable. The system that they attempt to control is a of a 4^{th} order and they only have three parameters k_p, k_i and k_d to control them with. Thus, they are restricted in the placement of the poles and must assume that the real part of the pole remains constant.

We also want to design the controller for the higher order system directly instead of first designing for the rigid case and then incorporating flexible modes later. If we consider only the rigid case along with the actuator, the open loop system is basically a third order system (3 poles and 1 zeros).

Now if we incorporate the flexible modes we notice that an equal number of poles and zeros are added to the system due to which the difference between the number of zeros and poles is still the same. Thus, the class of higher order systems we are concerned with can be written as:

$$G(s)=\frac{(s+z_1)(s+z_2)...(s+z_{n-x})}{(s+p_1)(s+p_2)...(s+p_n)} \quad (2\text{-}14)$$

where x is either 2 or 3. This means that we want to develop a controller for higher order systems where the difference between the poles and zeros is either 2 or 3. In its simplest form when the system has no zeros, thus the system reduces to a second/third order system with no zeros. There are several methods to control second order systems in literature, we focus our attention on controlling third order systems and then extending our work to the higher order system that we consider in Eq. (2-14).

Note that we are focused on single axis attitude control of flexible spacecraft since our approach works on SISO systems. We assume that the coupling on each of the axis is minimal.

2.6 Proportional-Integral-Derivative-Acceleration Controller

There are a few ways to control a third order system like the one presented in Eq. (2-13) using a PIDA (proportional integral derivative acceleration) system as well in literature. One of the ways is to determine dominant pole locations based on desired performance characteristics, then use PIDA feedback. One of the design methods places the poles in their desired locations by identifying gain values such that the closed loop characteristic equation coefficients are equated to those of the desired characteristic equation [5]. In [5], the authors address the fact that using a PID is inherently unstable for third order systems and the introduction of acceleration feedback stabilizes the root locus of the system as can be seen in Figure 1-2. A second method is to adjust the closed loop gain appropriately till the desired pole locations lie on the root locus [6]. In [21] a design for a mems based 3-axis accelerometer is shown, which shows us that it is imperative that we investigate how

to make better controllers based on acceleration feedback itself rather than filtering the signal and using it for position feedback. In [25] the authors have designed an acceleration feedback control for direct drive motor systems. Their control system is designed on 3 principles: i) no roots in the right half plane, ii) reducing the dynamic disturbance by limiting the bandwidth and iii) keeping the phase lag within a specified boundary. In [26], the authors show a discrete-time PIDA controller designed by Kitti's method which is references in [6]. In [27] the author's design an optimal design algorithm to find the parameters of the PIDA controller. In [28] the authors provide a method to auto-tune a PID and PIDA controller for a time-delayed second order system. In [29] the authors have presented a robust PIDA control scheme for load frequency control of interconnected power systems. In [30] the authors provide an auto-tuning method to find the gains of PIDA controller based on gain margin and phase margin. In [31] an optimal design of PIDA controller using harmony search algorithm for AVR power systems was developed. In [32] the authors have provided an acceleration feedback procedure to control vibration of aerospace structures.

These controllers assume no system zeros, which can radically affect the transient response of the system, and thus the dominant poles will not be the only factors to be considered when designing the system. The other problem with these controllers is that if the equations relating the pole positions to the system response are incorrect there is no other way to robustly assign control gain values to improve the system response.

Chapter 3 PROPORTIONAL DERIVATIVE ACCELERATION CONTROLLER DESIGN

Summary: In this chapter we show how to tune a PDA controller for a third order system, we then show the stability of the system when the controller is used, we show how the controller can be used with a numerical example and then compare the results with regular PD control.

3.1 Theory of PDA & PIDA controller

Consider a third order model in the frequency domain,

$$\frac{Y(s)}{U(s)}=G(s)=\frac{1}{(s+a)(s^2+2\xi\omega s+\omega^2)} \tag{3-1}$$

We want to design a PDA controller that provides a response according to specifications. Let $e(t)=y_d(t)-y(t)$, where $e(t)$ is the error between the desired response $y_d(t)$ and measured response $y(t)$.

Similarly,

$$\ddot{e}(t)=\ddot{y}_d(t)-\ddot{y}(t), \tag{3-2}$$

$$\ddot{e}(t)=\ddot{y}_d(t)-\ddot{y}(t), \tag{3-3}$$

The form of a PDA controller in the time domain is as follows:

$$u(t)=k_a\ddot{e}(t)+k_d\dot{e}(t)+k_p e(t) \tag{3-4}$$

Applying Laplace transform to Eq. (14), we get

$$C(s)=\frac{U(s)}{E(s)}=k_a s^2+k_d s+k_p, \tag{3-5}$$

where k_a is the acceleration gain, k_d is the derivative gain and k_p is the proportional gain.

It should be noted here that implementing the controller as presented in Eqs. (3-5) is not ideal since high frequency noise gets amplified due to the derivative and acceleration terms. Instead we implement a filter to cut-off the high frequency noise, thus making the transfer function look becomes:

$$C(s)=\frac{N_1 N_2 k_a s^2}{(s+N_1)(s+N_2)}+\frac{N_1 k_d s}{(s+N_1)}+k_p \tag{3-6}$$

where the values N_1 and N_2 can be simply tuned to be very high so that the controller in Eqs. (3-6) can be simply be written in the form presented in Eqs. (3-5) for the rest of this paper. This will not lead to ideal results every time since the controller will not behave as expected, thus we show 2 ways of assigning the gain values for the PDA controller.

Method 1:

In this case we assume that selecting a high enough filter value for N_1 and N_2 in Eq. (3-6) will produce a controller of the form of Eq. (3-5). The PDA controller can then be written as the product of two zeros as:

$$C(s)=K(s+z_1)(s+z_2) \tag{3-7}$$

where $z_1$and z_2 are the two zeros added to the closed loop system and K is the root locus gain. Thus, the design of a PDA controller involves tuning the parameters K, z_1 and z_2 such that the transient and steady state error specifications are met. Equations (3-7) and (3-5) are related as follows:

$$k_a=K \tag{3-8}$$

$$k_d=K(z_1+z_2) \tag{3-9}$$

$$k_p=Kz_1z_2, \tag{3-10}$$

This method is an ideal case and can be utilized for theoretical purposes when designing a

feasible controller for the system.

Method 2:

When working with a practical controller we must assign values for filters as provided in Eq. (3-6). Assume that we assign a value of N_1 and N_2 that is large enough such that the poles of the controller are far in the left half plane and thus do not contribute to the transient response of the system. Thus Eq. (3-6) can be approximated by

$$C(s) \approx (N_1N_2k_a+N_1k_d+k_p)s^2+\{N_1N_2k_d+k_p(N_1+N_2)\}s+k_pN_1N_2 \quad (3\text{-}11)$$

Thus equating (3-11) with (3-7) we get

$$k_p=\frac{Kz_1z_2}{N_1N_2}, \quad (3\text{-}12)$$

$$k_d=\frac{K(z_1+z_2)-k_p(N_1+N_2)}{N_1N_2}, \quad (3\text{-}13)$$

$$k_a=\frac{K-N_1k_d-k_p}{N_1N_2}, \quad (3\text{-}14)$$

When implementing a controller using PDA, it is imperative that we assign the gain values as mentioned in Eq. (3-12) to (3-15). For the remainder of the theory section however we continue to use Eq. (3-8) to (3-10) since it will help us establish some conditions for stability and controller design without having to deal with complex algebra.

The root locus of the system begins from the characteristic equation where C(s) is the compensator transfer function and G(s) is the open loop model of the system

$$1+C(s)G(s)=0 \quad (3\text{-}15)$$

$$1+\frac{K(s+z_1)(s+z_2)}{(s+a)(s+p_1)(s+p_2)}=0, \quad (3\text{-}16)$$

where a is the real pole, p_1 and p_2 are the complex conjugate poles. It is clear from Eq. (3-16) that if z_1 is placed at 'a' or close to 'a' the system can be reduced to a second order

system, as we are cancelling the real pole by placing a zero on or close to it. The system is now effectively reduced to a second order system with one zero by pole-zero cancellation and the design is therefore reduced to adjusting z_2 such that the two dominant poles are placed where they provide a satisfactory response. We will use this feature to design our tuning procedure in Section 3.3.

For certain systems, simply providing a proportional gain does not lead to zero steady state error, and thus for these cases we must include an integrator in the system. Thus, the compensator can now be written as

$$u(t)=k_a\ddot{e}(t)+k_d\dot{e}(t)+k_pe(t)+k_i\int e(t) \tag{3-17}$$

which in the frequency domain is

$$C(s)=\frac{k_as^3+k_ds^2+k_ps+k_i}{s} \tag{3-18}$$

3.2 Stability of PDA and PIDA System

The stability of the compensated system is of fundamental importance, and this is evaluated through expanding the characteristic polynomial. Let C(s) be the compensator and G(s) be the open loop model of the system, then the closed loop system is written as

$$G_c(s)=\frac{C(s)G(s)}{1+C(s)G(s)} \tag{3-19}$$

The denominator of Eq. (3-19) is called the characteristic equation of the system. Taking Eq. (3-7) for C(s) and Eq. (3-1) for G(s), and substituting in Eq. (3-19) above, the denominator becomes

$$s^3+(a+2\xi\omega+k_a)s^2+(\omega^2+2\xi\omega a+k_d)s+(a\omega^2+k_p)=0, \tag{3-20}$$

We can see in Eq. (3-20) that the system is of 3rd order and we have three parameters k_p,

k_d and k_a to control each of the parameters with. Thus, if we were to utilize the same technique of pole placement as in [1] and [2] we will have better control of the placement of the poles. It is difficult to estimate where the placement of the poles would result in a desired transient response for a flexible spacecraft, thus we will avoid using that technique and choose a tuning procedure as outlined in section 3.3.

Applying the Routh Hurwitz criterion to the Eq. (3-20) we arrive at three conditions for the gains such that the poles are unconditionally stable.

Conditions:

1. $k_a > -(a+2\xi\omega)$
2. $k_d > -(\omega^2 + 2\xi\omega a)$
3. $k_p < (a+2\xi\omega+\kappa_\alpha)(\omega^2 + 2\xi\omega a + k_d) - a\omega^2$

If these conditions are met for the gains, the system response will asymptotically decay to zero i.e. the poles of the closed loop system $G_c(s)$ will be placed in the left half plane.

When the integrator is also added to the control input, like in Eq. (3-18), the stability conditions are modified as follows:

Conditions:

1. $k_a > -(a+2\xi\omega)$
2. $k_i > 0$
3. $k_d > \dfrac{(a+2\xi\omega+k_a)k_i + (a\omega^2+k_p)^3}{(a+2\xi\omega+k_a)(a\omega^2+k_p)} - (2\xi\omega+\omega^2)$
4. $k_p > (a+2\xi\omega+k_a)(\omega^2+2\xi\omega a+k_d) - a\omega^2$

3.3 Tuning Procedure

The detailed tuning procedure is laid out in the following steps:

Place z_1 at -a to cancel out the real pole. Observe the step response of the system. Note the rise time, settling time, over shoot and steady state error of the step response.

If a is at the origin then to maintain zero steady state error, place the real zero z_1 to the left of the origin depending on the positions of the complex poles then follow step 3.

1. The location of z_2 is then found through the following procedure:
2. z_2=-ap$_{z1}$, where a is the real root and p_{z1} is the ratio between the final position of the second zero and the real root. Increase this value until settling time no longer increases.
3. Increase the root locus gain K till the desired overshoot and settling time value is achieved. If the compensator is unable to meet the steady state requirements, the design procedure must begin anew, this time by adding an integrator in the system as outlined in step 5.
4. $C(s)=\frac{k_a s^3+k_d s^2+k_p s+k_i}{s}$, where the objective is to assign three zeros, z_1=-a, z_2=-ap$_{z1}$ and z_3=-p$_{z2}$ The idea behind this is to place the zero z_3 close to the integrator so we assign p_{z2} to be a small value. We then design the remaining zeros as in step 1-3. Thus, we can improve the response and the integrator pole will help us meet our steady state requirements.

3.4 Numerical Example

Consider an example shown in Figure 3-1. It is provided of how a third order system can be realised. We consider a first order motor with a real pole at $-\omega_m$ and a second order flexible link with damping ratio ξ and natural frequency ω. Thus, the system in Eq. (3-1) becomes

$$\frac{Y(s)}{U(s)}=\frac{1}{(s+\omega_m)(s^2+2\xi\omega s+\omega^2)} \tag{3-21}$$

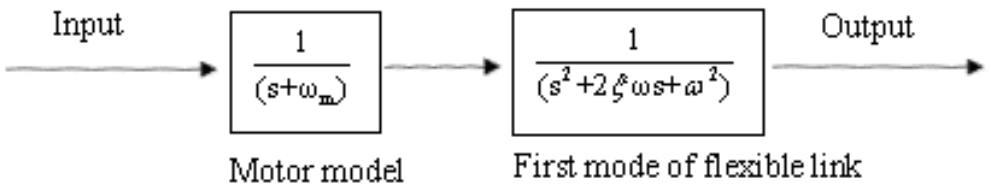

Figure 3-1: Third order open loop system practical example block diagram.

Let ω_m be -3, ξ be 0.2 and ω be 1, thus we have one real pole at -3 and a complex conjugate pair at $0.2 \pm 0.9798i$. The unit step response of the open loop system is shown in Figure 3-2 (blue line).

Let the desired specifications be (arbitrarily):

1. Settling Time, T_s<1s, where T_s is the time it takes for the signal to reach its steady state response.
2. Overshoot Percentage, $OS\% \leq 16\%$, where OS% is the percentage that the output exceeds its desired response.

The steps as outlined above in section 3.3 are followed to develop a controller for the third order system:

1. Place one of the zeros on the real pole, thus z_1=3. Let, p_z =1, placing the second zero at z_2=-6. The settling time T_s, is 5.152s
2. The zero is placed far enough into the left half plane and increasing it further increases the settling time rather than reducing it, so we move on to increasing the gain till the desired specifications are met.

3. Now we modify the gain of the system till we meet the overshoot specifications. Let,

   K = 1, T_s=5.152, OS% = 46.8289

   K = 10, T_s=0.6201s, OS% = 21.3689

   K = 35, T_s=0.3821s, OS% = 9.8911

Thus, we have met our desired specifications of a faster settling time and brought the overshoot value to below 16% The results can be seen in Figure 3-2. In Figure 3-3 it is also shown how one can use a practical realization of this controller using Simulink and the step response is shown to be very close to the one developed above in Figure 3-4.

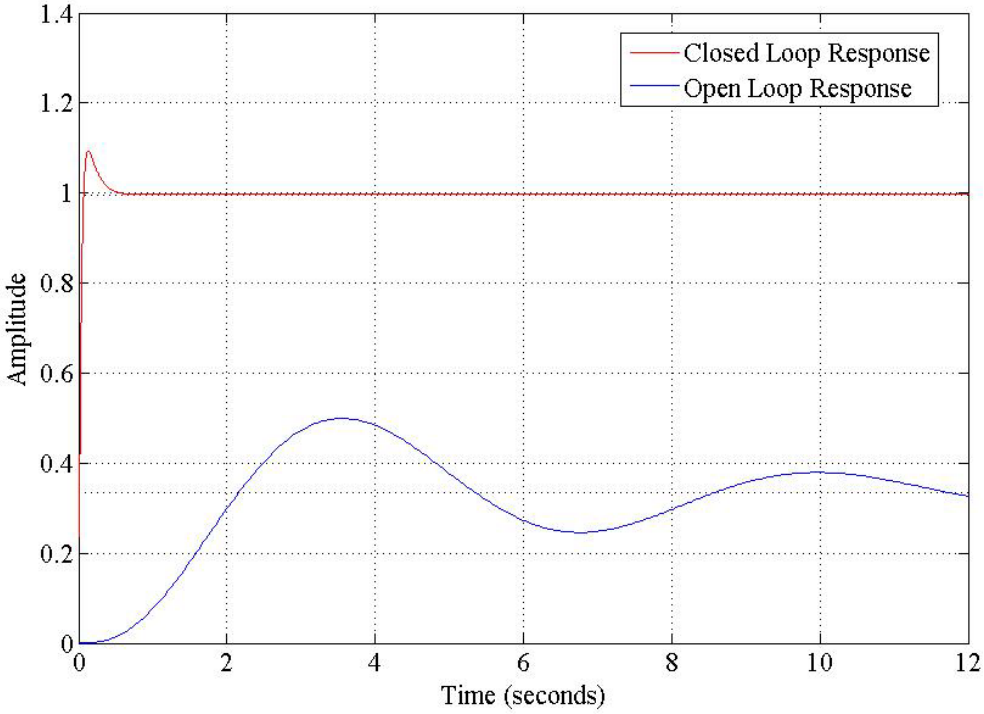

Figure 3-2: (Blue)Step response of open loop system. (Red) Step Response of closed loop system.

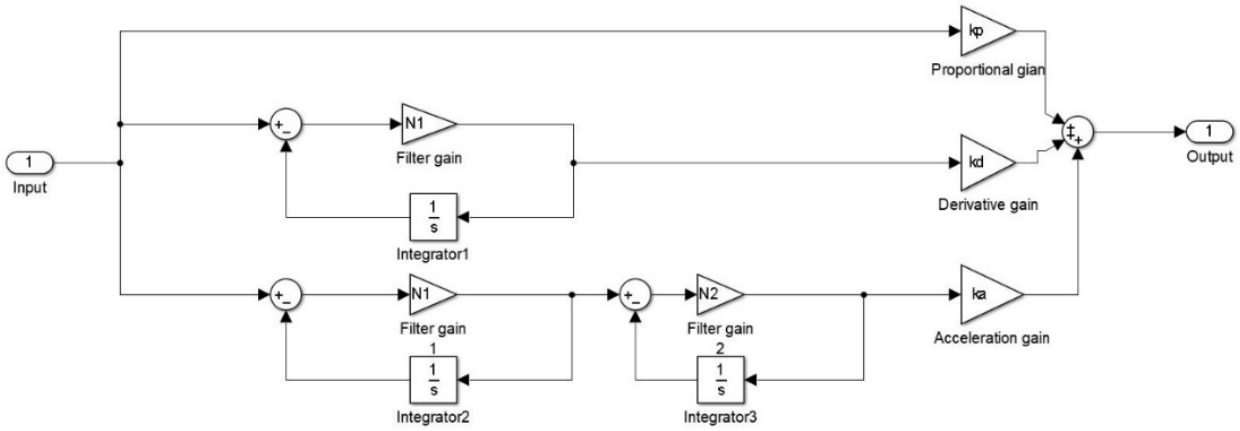

Figure 3-3: Practical realization of the PDA controller.

In Figure 3-3, we choose the values of N_1 and N_2 to be 140, thus the filter cuts-off higher frequency noise at $2\pi N_1$ and $2\pi(N_1+N_2)$ so that the block can simulate the response of a differentiator and acceleration signal and filter out higher frequency noise. It can also be observed that in Figure 3-4, the step response has a larger overshoot than Fig. 3-2 which validates that the controller works in practical implementations. The value of N_1 and N_2 is chosen to be 140 because it is low enough so that we can filter out all the higher frequency noise above $2\pi N_1$ and large enough to function as a differentiator and accelerator.

3.5 Comparison to PD Control

In Figures 3-4 and 3-5 we plot the step response of the system in the numerical example discussed above using the PDA controller developed in Simulink and the PID controller in Simulink respectively. We demonstrate how the PDA controller does give a better response with faster settling time. We also demonstrate a practical realisation of the controller can be formed by introducing a filter before the derivative and acceleration gains.

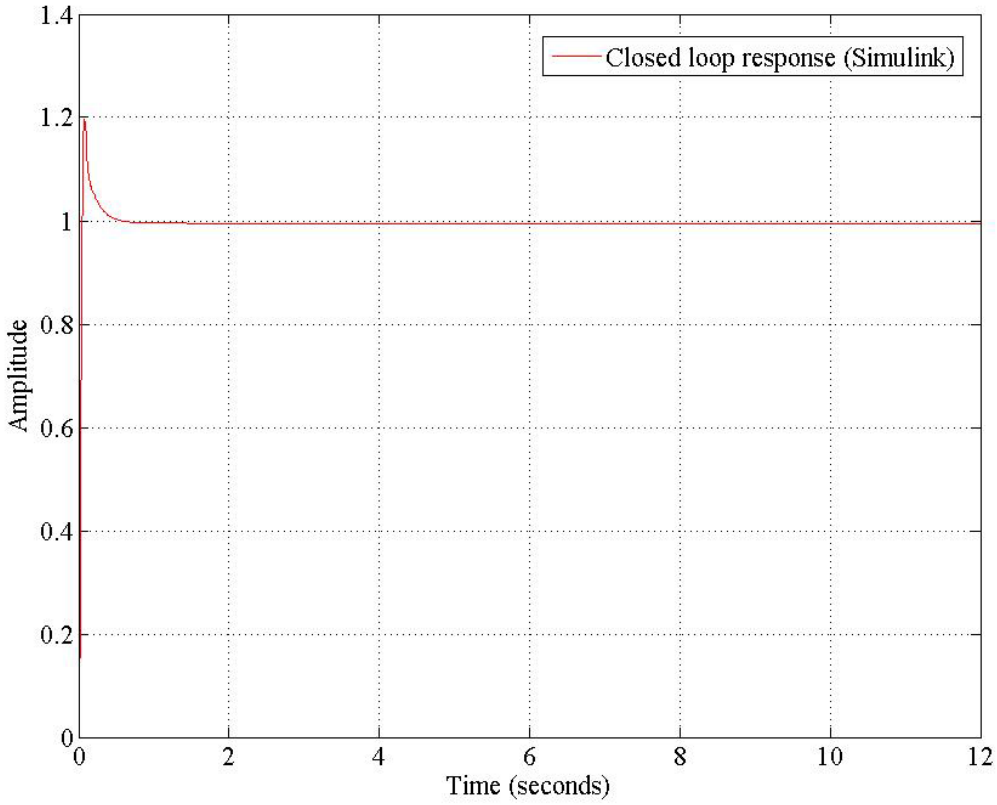

Figure 3-4: Step Response of closed loop system using PDA for the example in section 3.4 performed in Simulink.

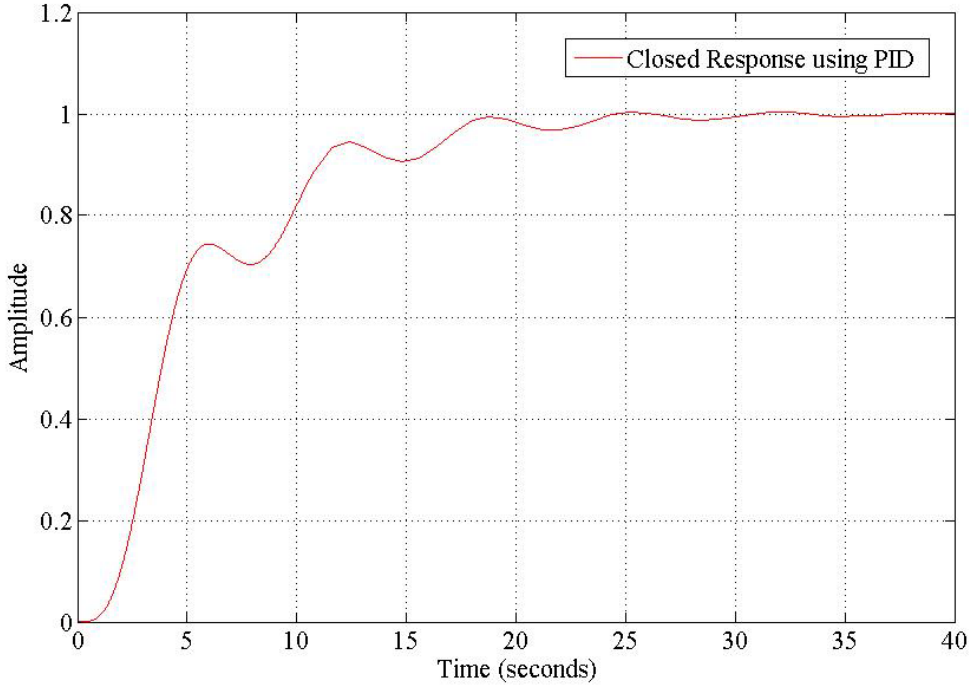

Figure 3-5: Step Response of closed loop system using PID for the same system in Section 3.4.

Chapter 4 FLEXIBLE LINK EXPERIMENT

Summary: In this chapter the experimental setup is described, then the model estimation procedure is showcased, then a PDA controller is designed, and its results are discussed.

4.1 Experimental Setup

The flow chart for the experimental setup is outlined in Figure 4-1

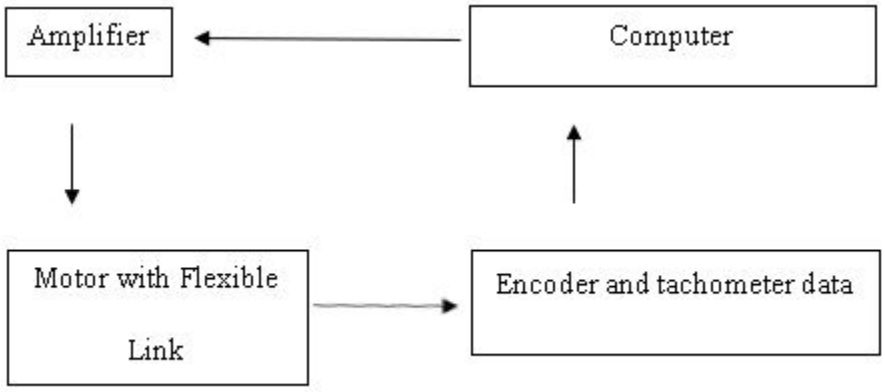

Figure 4-1: Flow chart representing the experimental setup.

The setup consisted of a Quanser rotary flexible link and an SRV-02 motor. This was attached to an amplifier which was hooked onto a computer where we apply the controller. The sensors in the setup are a tachometer and encoder which measure the angular rate and angle that the motor spins. To feedback acceleration we must differentiate the signal from the tachometer with time once. As specified in section 3, we added filters on the differentiated signal so that the system is causal. This setup was chosen because the motor can be represented as a first or second order system and the flexible link can be modelled as a second order system. In conjunction this can be represented as a fourth order

or third order system. Since this is the sort of system we are trying to control, we compare our approach to a PID and observe any improvements.

To verify if acceleration feedback would help improve the response of the system, we first perform an experiment wherein we add acceleration feedback to regular PD control and observe any improvement in the transient response of the system

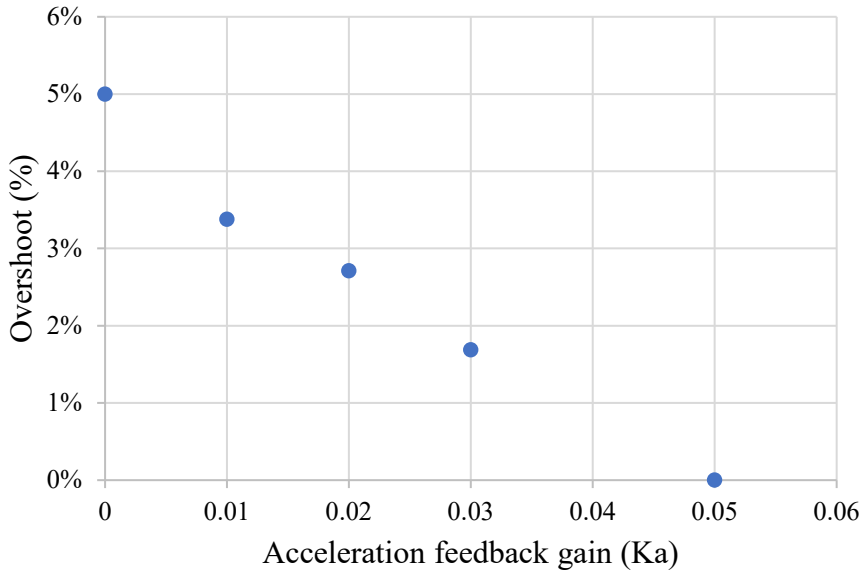

Figure 4-2: Overshoot vs acceleration feedback gain.

In Figure 4-2, we can see that the overshoot has improved considerably as the acceleration feedback gain is increased.

4.2 Model Estimation for Flexible Link Setup

To apply PID or PDA control to the flexible link, we first estimated the transfer function between the control input and the angle that the flexible link rotated. We did this by sending a step input in the system and observing the response. The data points collected were then used by MATLAB's tfest() function to estimate the poles and zeros of the system. The transfer function between the voltage applied to the motor and the angular velocity of the

flexible link was estimated to be a 4th order system with a time delay of 0.08 seconds.

$$G(s)=\frac{6.645e06s^2+2.792e08s+7.463e10}{s^4+2.39e04s^3+3.92e06s^2+7.21e08s+4.553e10} \quad (4\text{-}1)$$

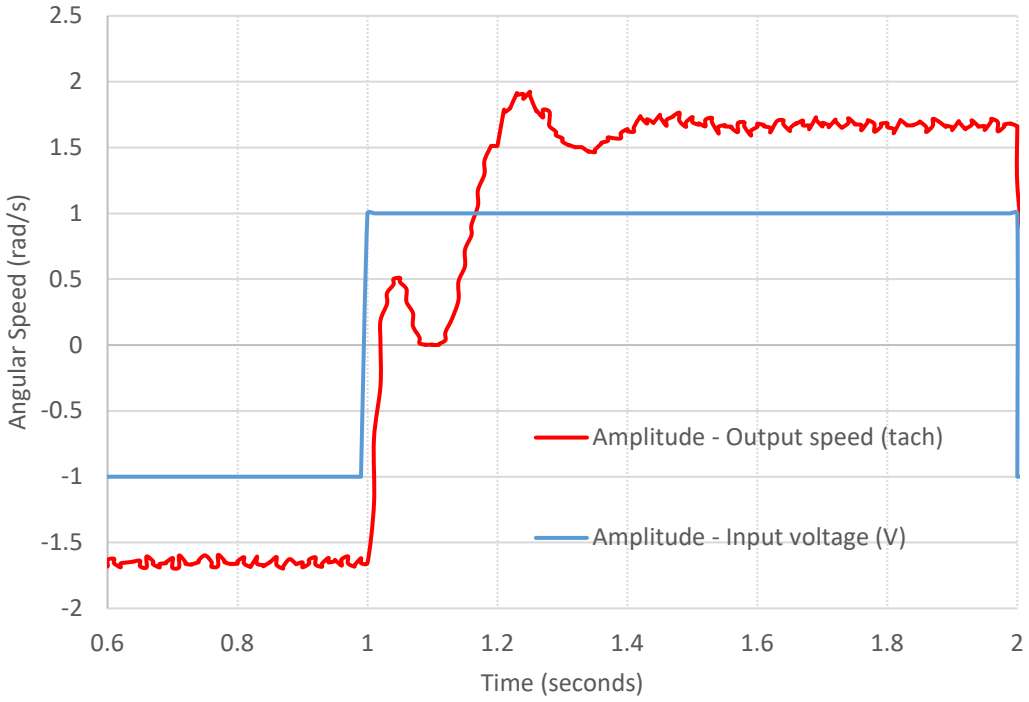

Figure 4-3: Open loop step response of the flexible link system.

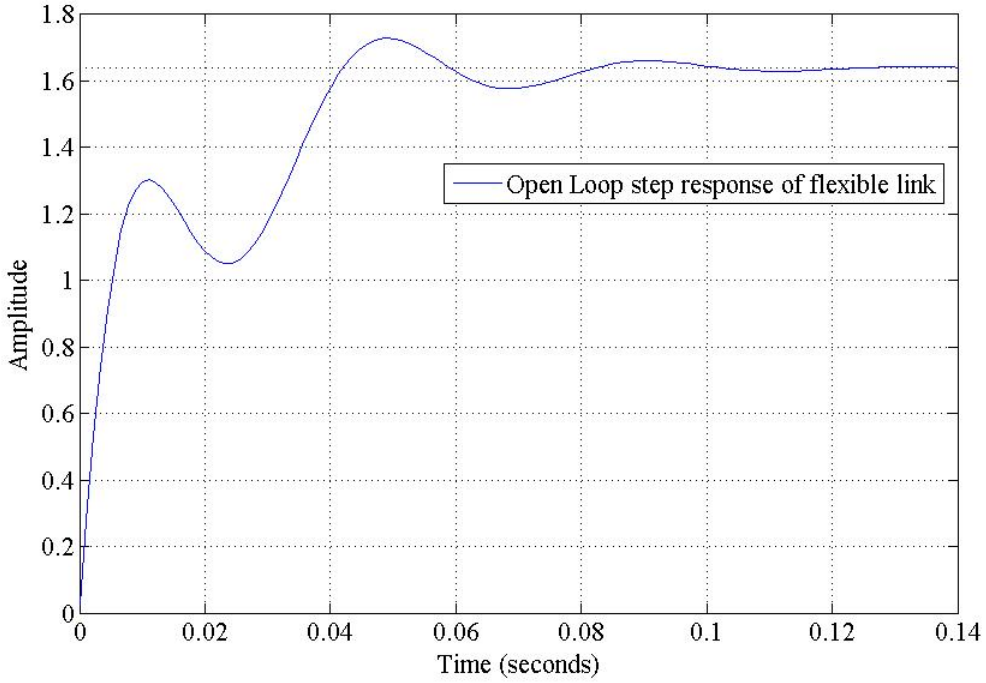

Figure 4-4: Step response of the estimated transfer function from Eq. (4-1).

When we compare Figures (4-4) and (4-3) we can see that the estimated transfer function response in Eq. 4-1 follows the open loop response of the flexible link setup. The system response might be a little slower than the simulated response due to nonlinear effects arising from the gear contact between the motors and the flexible link. These cannot be modelled by MATLAB's tfest() function.

To estimate the response between the angle and voltage applied we included an integrator and a gain. Thus, the net transfer function is as follows:

$$G(s)=\frac{\theta(s)}{V(s)}=\frac{60(6.645e06s^2+2.792e8s+7.463e10)}{s(s^4+2.39e04s^3+3.92e6s^2+7.21e08+4.553e10)} \quad (4\text{-}2)$$

Since this is a fifth order system with 2 zeros we can design a PDA controller to improve the response of the system and ensure that the transfer function is proper. This is theoretically possible since we will try to design a controller where we place one of the

zeros on the real pole and then place the other zero so that the one of the remaining poles will decay into its respective zero and one would be driven to infinity.

4.3 PDA Controller Design

When applying PDA control from section 3.3, we attempt to place one of the zero on the real pole of the open loop system. The real pole here is at zero, thus we do not want to cancel out the response of that pole by placing the zero on it as it will negate the zero steady state error. To solve this problem, we try placing the zero on the real part of one of the complex poles, but the gains required to place them there are too high since the zeros are placed too far in the left half plane.

Thus, we arbitrarily place one of the zeros in the left half plane and then proceed with step 2 in section 3.3 to place the other zero and then adjust the gain till the response is satisfied. The zeros are placed at z_1=-5.9390 and z_2=-4.3174. The filtering factor is chosen to be 10 by trial and error. The root locus gain was selected to be 1. The simulated response is provided in Figure 12. This showcases the flexibility of our tuning procedure as we are not restricted to choosing poles and zeros to work with, rather we can place the zeros on the left half plane and adjust the gain till the desired response is obtained.

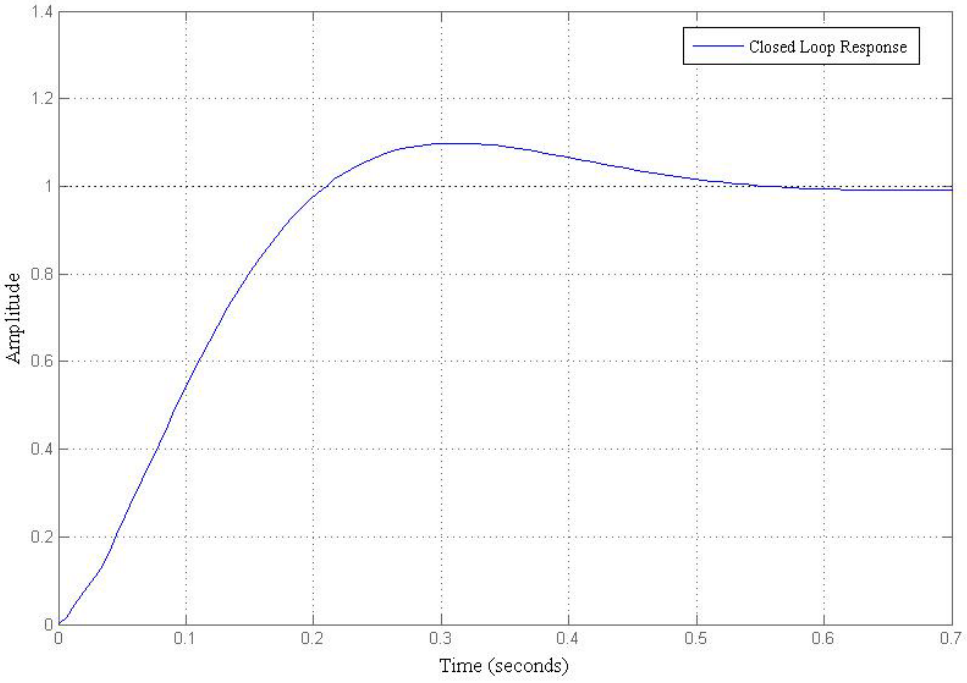

Figure 4-5: Step response of the simulation of the flexible link.

The response of the experimental setup is provided in Figure 4-5. As can be seen the response time is like the estimated simulated response. The oscillations that can be seen in Figure 4-6 can be attributed to some nonlinear effects and such that were unmodeled in the open loop system response in Eq. (4-2). The settling time is 1 second and Overshoot is around 1.67%.

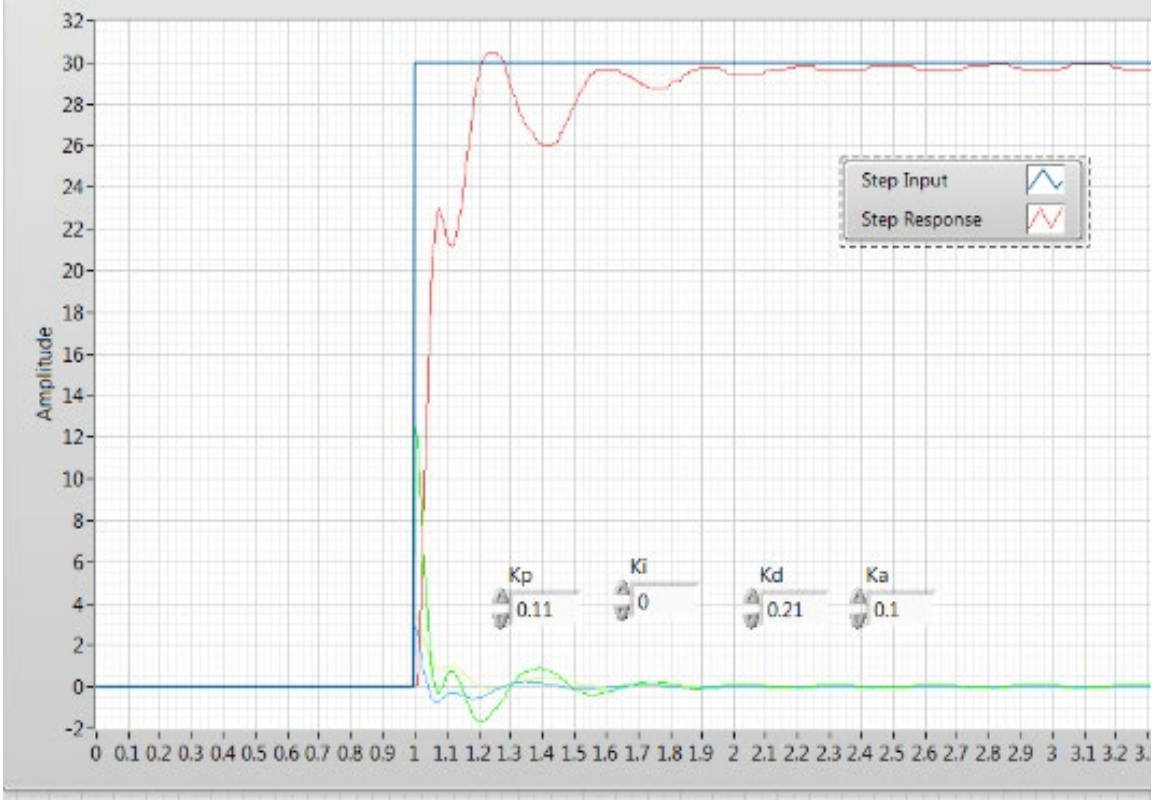

Figure 4-6: Response of the flexible link to the PDA controller.

4.4 Manual Tuning of PDA

In Figure 14 we show the results of manually tuning the PDA controller, where we can obtain a response with less oscillations by simply reducing the derivative gain a little.

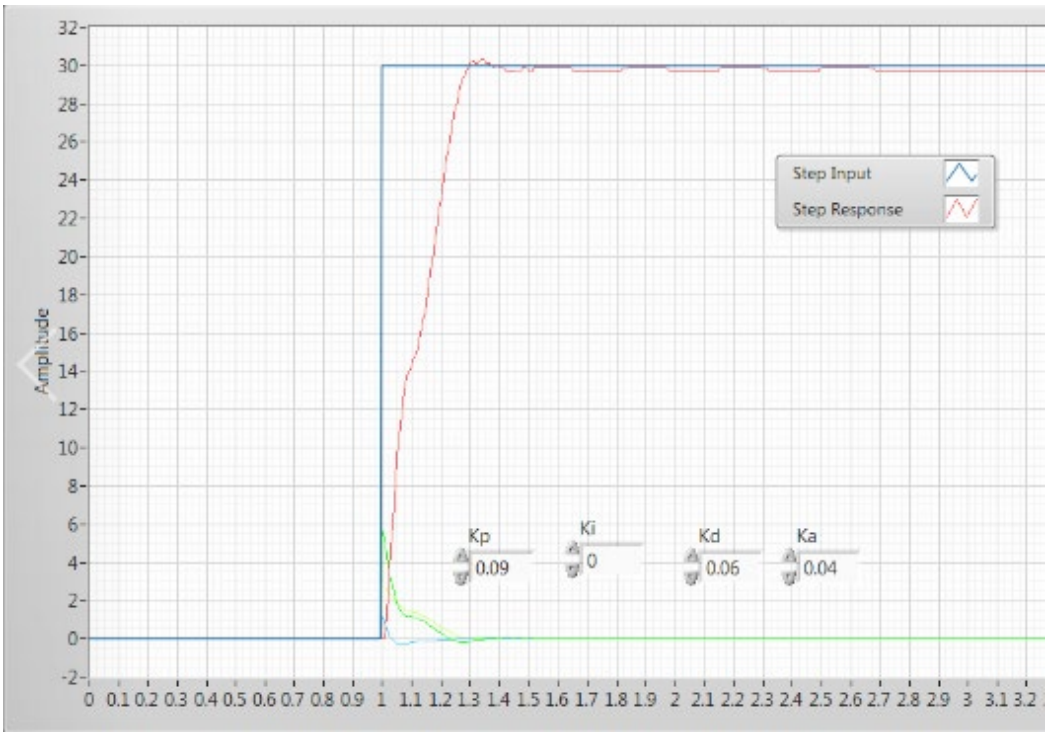

Figure 4-7: Response of the flexible link setup to manually tuned PDA controller.

4.5 Comparison to PID Controller

The PID control parameters were chosen to be k_p=0.1, k_i=0.0015, k_d=0.05, the tuning was performed in MATLAB's Simulink. In [22] a comprehensive study of different PID tuning techniques is provided. We use Simulink's tuning procedure as it is widely used and easy to modify as the parameters are varied. The settling time is 0.7 second and Overshoot is around 6.67%. We can see that PDA controller provides a better response than PID.

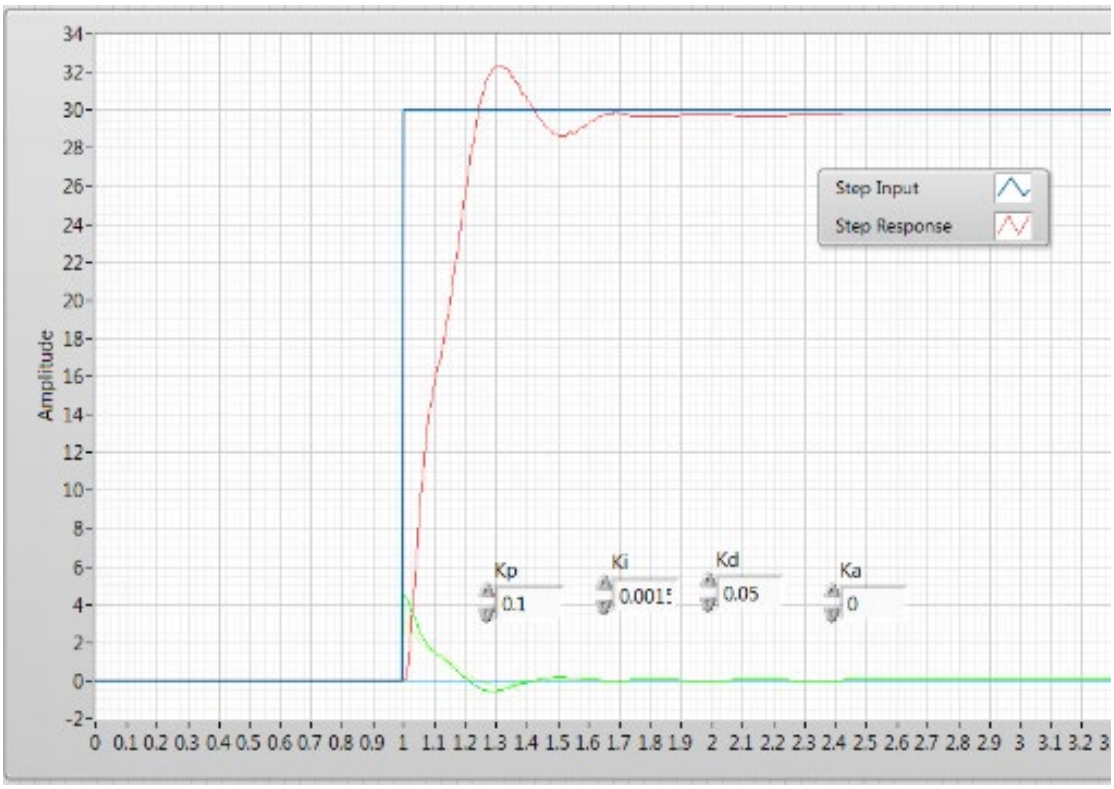

Figure 4-8: Response of the flexible link to the PID controller.

Chapter 5 SINGLE AXIS ATTITUDE CONTROL OF FLEXIBLE SPACECRAFT

Summary: We now turn our attention to attitude control of a generic spacecraft consisting of a rigid hub with flexible appendages represented by an arbitrary number of modes. The compensator of Section 3 above is adapted for this model, then applied to a specific example.

5.1 Rigid Body Spacecraft Control

The rigid body model of the spacecraft consists of a rigid body and actuator dynamics, where A(s) is the actuator model, S(s) is the sensor model and R(s) is the rigid body model as defined in Section 2.1.

Thus, the open loop model of the system is,

$$\frac{\theta(s)}{u(s)}=H(s)=A(s)R(s) \tag{5-1}$$

In [1], it is noted that sensors and actuators have a lag term associated with them, i.e., they are not ideal. Thus $\omega_a(=\frac{1}{\tau_a})$ is a characteristic of the actuator where τ_a is the actuator time lag and $\omega_s(=\frac{1}{\tau_s})$ is a similar figure associated with the sensor with τ_s its time lag. Thus, the sensor model can be written as:

$$S(s)=\frac{1}{(s+\omega_a)} \tag{5-2}$$

In Section 2.1 we have assumed that the actuator is of a first order model and the rigid body is of second order.

$$\frac{\theta(s)}{u(s)} = \frac{s}{Is^2(s+\omega_a)} \tag{5-3}$$

We also include the sensor model in our system as shown in Figure 2-4. When designing the placement of the zeros we only concern ourselves with the model presented in Eq. (5-3). The root locus of this system is derived by

$$1+H(s)S(s)=0, \tag{5-4}$$

where H(s) is defined in Eq. (5-1) and S(s) in Eq. (5-2). In Appendix 1 we have provided the parameters we used to model the spacecraft from Eq. (5-2). Since the motivation for this research comes from expanding the work done in [1] and [2] we also chose the same spacecraft (CTS) to verify our design procedure so we can compare our results with the ones the authors before us achieved. We then use the procedure from section 3.3 to design a PDA controller for the system in Eq. (5-3).

The system is essentially a third order system with two poles at the origin and one real pole at $-\omega_a$.

5.2 PDA Controller Design

To design a PDA controller, we first choose the placement of the zeros and then adjust the root locus gain K until the overshoot and settling time requirements are met. It should be noted here that implementing a PDA controller for rigid body spacecraft means that we are able to feedback the angle position, angular rate and angular acceleration to the controller. For the rigid body example considered, the following parameters are used:

Controller 1: $z_1 = -0.00026$, $z_2 = -26.003$ and $K = 40$.

In Figure 5-1 we present the root locus of the PDA controller with the rigid spacecraft

system by substituting the spacecraft parameters in Eq. (5-4). As presented before in Section 1.2, this reinforces the point that PDA is better suited to control third order and higher systems. The step response of the closed loop system with Controller 1 is given in Figure 5-2.

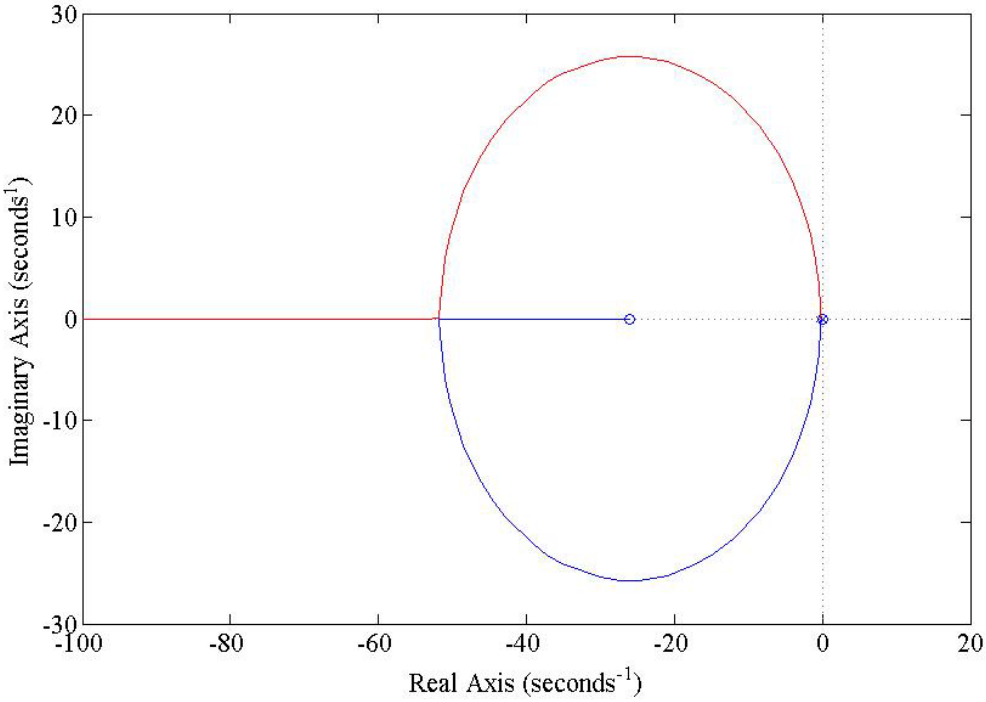

Figure 5-1: Root locus of the rigid body case with PDA controllers.

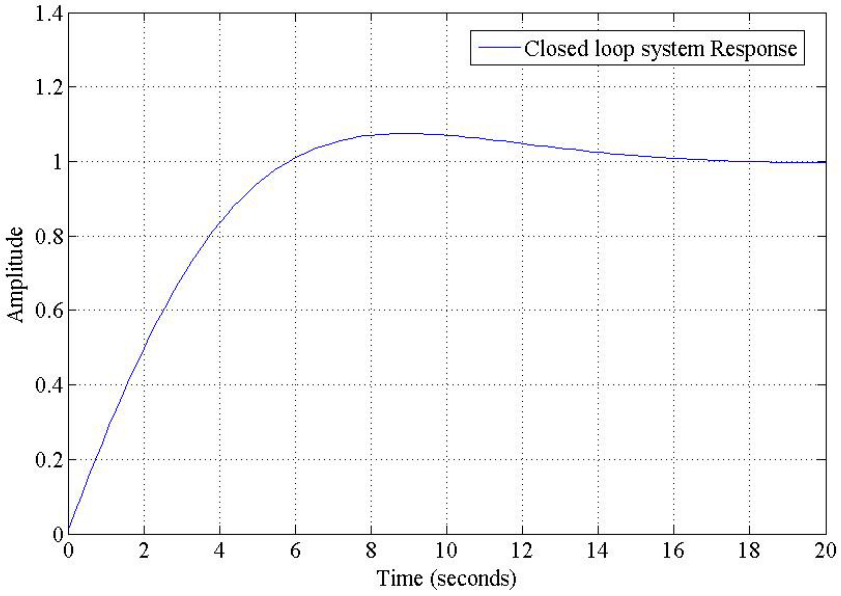

Figure 5-2: Rigid body case closed loop system response.

5.2 Flexible Appendage Control

We have presented the model of a flexible spacecraft in the literature review before in section 2.2. Considering the equations of motion Eq. (2-14) and (2-15), let us convert the equations from time to frequency using Laplace transform

$$Is^2\theta(s)+\sum h_n s^2 q_n(s)=T(s) \tag{5-5}$$

$$h_n\theta(s)+I_f q_n(s)\{s^2+2Z_n\Omega_n s+\Omega_n{}^2\}=0 \tag{5-6}$$

Isolating $q_n(s)$ in Eq. (5-6) and substituting in Eq. (5-5) we get

$$\frac{\theta(s)}{T(s)}=\frac{1}{I_e s^2} \tag{5-7}$$

where $I_e(s)$ is the inertance,

$$I_e(s)=I\left(1-\sum_n \frac{h_n s^2}{II_f(s^2+2Z_n\Omega_n s+\Omega_n{}^2)}\right) \tag{5-8}$$

We now gather all the flexible modes together and represent them by F(s) as:

$$F(s)=\sum_{i=1}^{n}\frac{s^2K_i}{s^2+2Z_i\Omega_i s+\Omega_i^{\,2}} \tag{5-9}$$

where n is the number of flexible modes and $K_i=\frac{h_n}{II_f}$.

Thus, we can write the inertance as

$$I_e(s)=I(1-F(s)) \tag{5-10}$$

Now the open loop transfer function from Eq. (5-7) becomes

$$\frac{\theta(s)}{T(s)}=\frac{1}{Is^2(1-F(s))} \tag{5-11}$$

This representation is much more tractable, and we can now represent the system in a block diagram as in Figure 5-3.

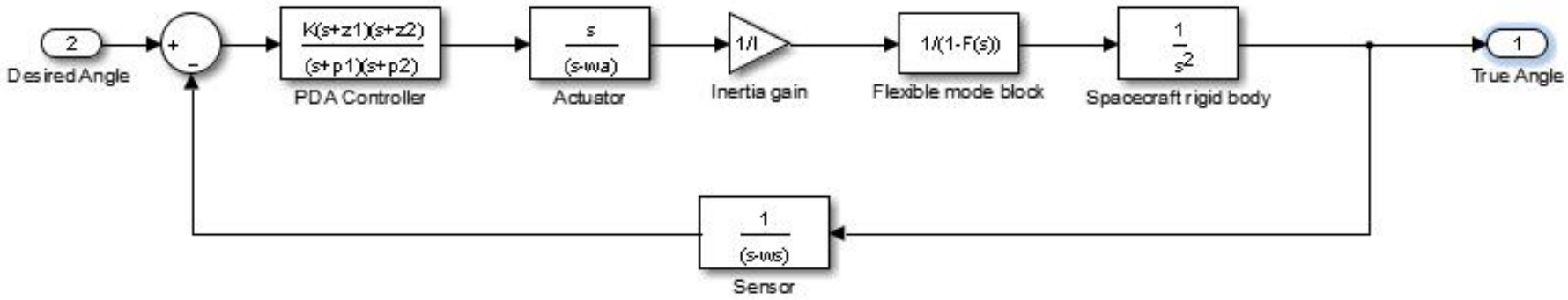

Figure 5-3: Simplified flexible spacecraft block diagram

The flexible mode block in Figure 5-3, introduces an equal number of poles and zeros in the system, thus the net difference between the poles and zeros is still caused by the rigid body modes. Since the net difference between the number of poles and zeros in the closed loop system remains the same, the design procedure in 5.1 can be applied. Keeping the same placement of zeros as in Section 5.1 we vary the gain till we achieve optimal transient characteristics. This is different from the rigid body case since the lightly damped flexible modes have an impact on the transient characteristics. This topic will be further developed in future research.

As the next step, this design procedure is applied to a model of a flexible spacecraft (CTS) of the early 1980s, whose parameters are listed in Table A1 of the Appendix 1.

As can be seen from Figure 5-4 the system root locus is very similar to that of the rigid body case in Figure 5-1. In Figure 5-5 we zoom into the long line of flexible modes presented in Figure 5-4.

It is seen that as the gain is increased the flexible modes approach their respective zeros. The poles are not completely cancelled by their respective zeros and thus they have an impact on the time response of the system.

Due to this the flexible poles contribute to the transient response of the system which is undesirable. Thus, we vary the gain K applied to the system until the desired transient response is achieved. For the CTS system provided in Appendix 1 [12], the PDA parameters used are:

Controller 2: $z_1 = -0.003$, $z_2 = -26.003$ and $K = 10$.

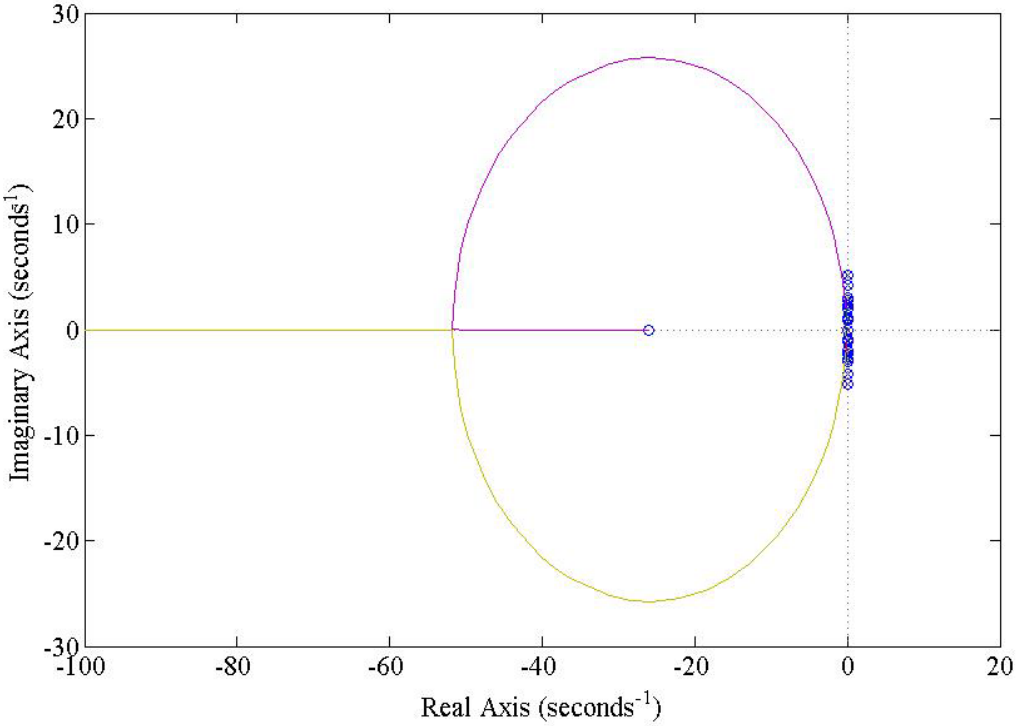

Figure 5-4: Root Locus of PDA controller applied to CTS Spacecraft

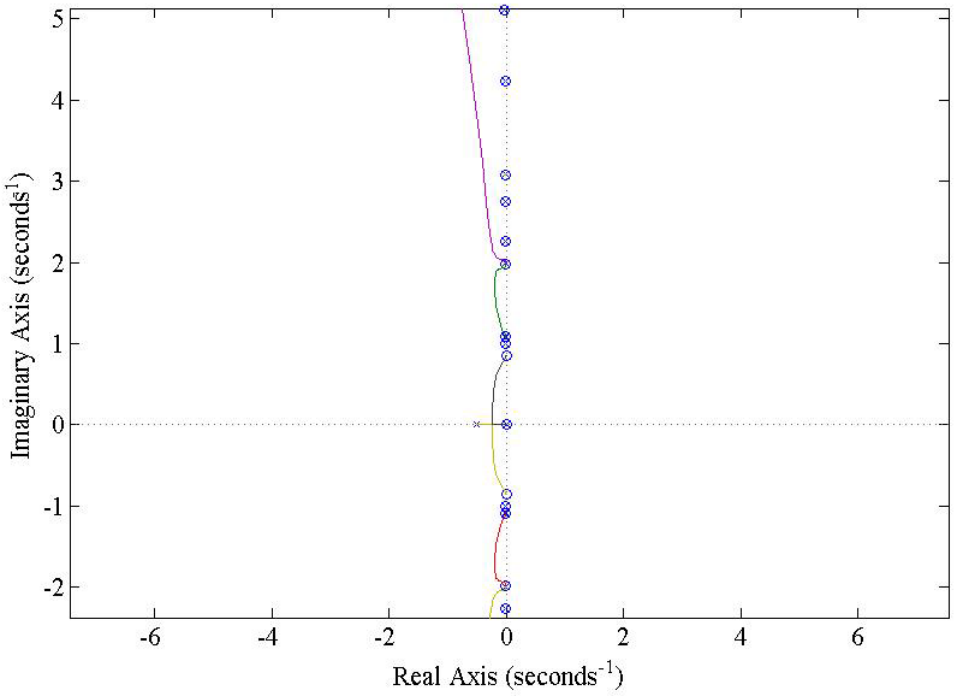

Figure 5-5: Root locus behaviour around the flexible mode region

In Figure 5-6, the PDA controller designed for the rigid body modes (Controller 1) was applied to the flexible spacecraft and the step response observed. As can be seen the flexible modes cause the time response of the system to become more oscillatory (undesirable). By simply varying the gain value we obtain PDA Controller 2 whose step response in Figure 5-7 is less oscillatory. The rise time, settling time and overshoot of the closed loop PDA controlled flexible spacecraft system are 82.850 seconds, 150.668 seconds and 0%.

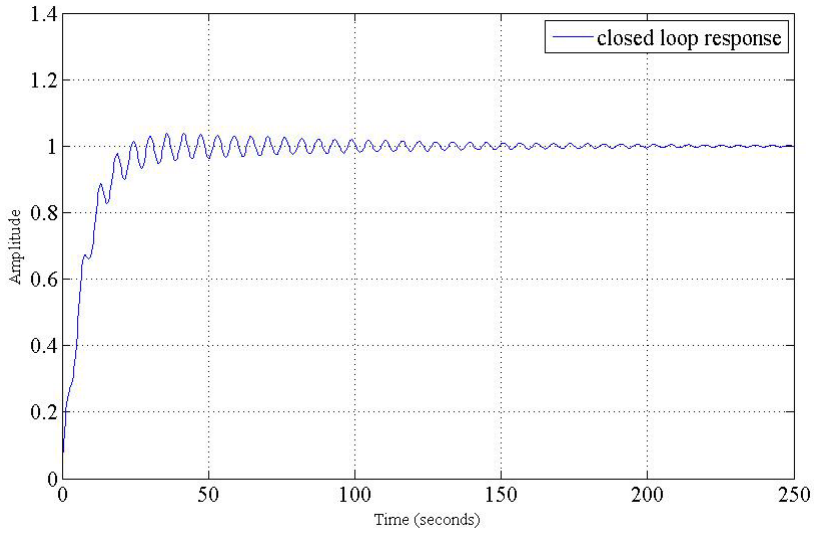

Figure 5-6: Step response of closed loop flexible spacecraft system with the PDA Controller 1

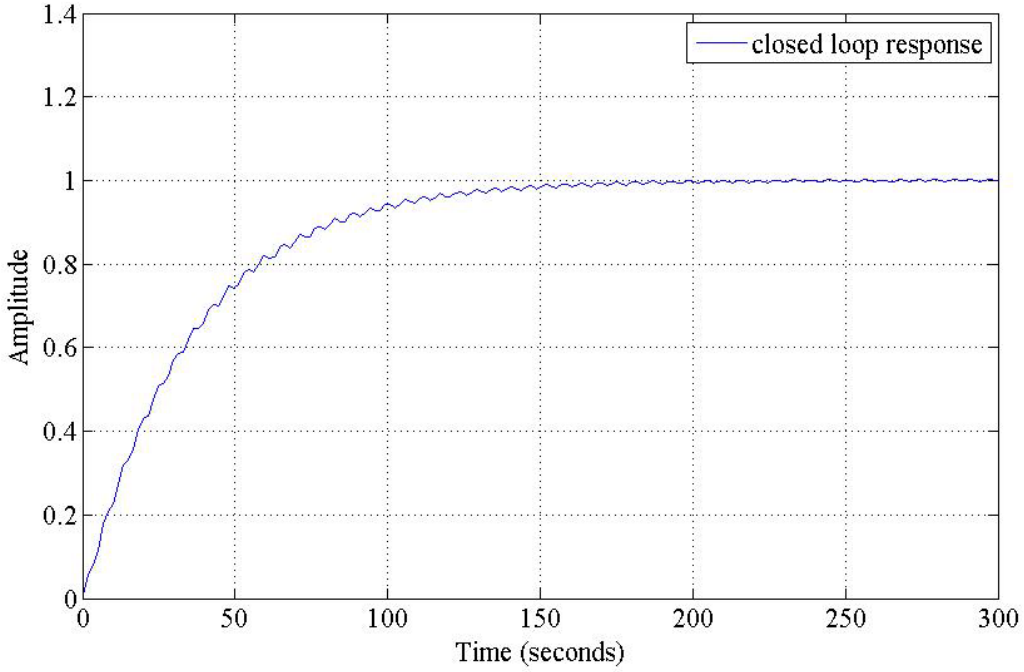

Figure 5-7: Step response of closed loop flexible spacecraft system with PDA Controller 2

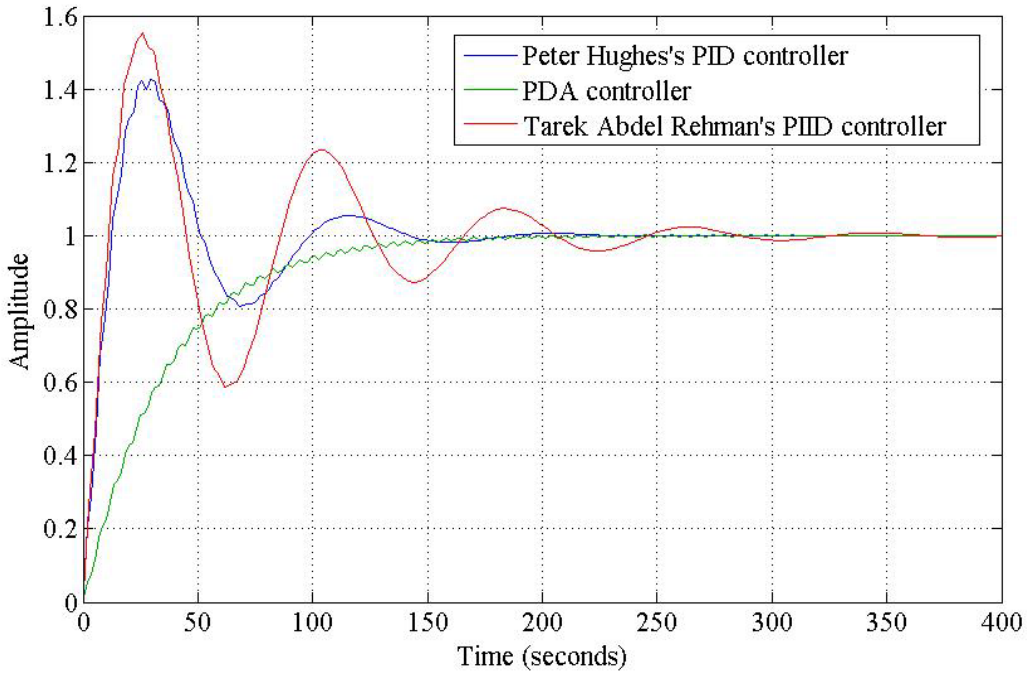

Figure 5-8: Comparison of the different controllers on the step response of the CTS spacecraft

In Figure 5-8, we plot Hughes' controller values developed in Hughes and Abdel-Rahman [1] and Abdel-Rahman's [2] PID values, and the PDA controller we developed. As can be observed our controller reduces the overshoot considerably.

The following are the characteristics of the PDA controlled (Controller 2) CTS spacecraft system:

Gain Margin = Infinite.

Phase Margin = 87.0489 degrees.

Gain crossover frequency=0.0263 rad/s.

In [1,2], it is mentioned that in order to avoid instability due to excitation of flexible modes, the frequency of the flexible modes should be above the phase crossover frequency. This way no flexible mode excitation will cause instability. In the PDA controller designed above, the phase of the system never crosses the -180 degree phase angle, thus the system gain margin is infinite (theoretical version). This the system is unconditionally stable for all flexible mode frequencies.

We also simulated the CTS spacecraft on Simulink using the block diagram in Figure 5-3, spacecraft parameters were used from [3], presented in Appendix 1. Controller 2 was then used to control the spacecraft and a filter value of 10 was used. The step response from the simulation is presented in Figure 5-9.

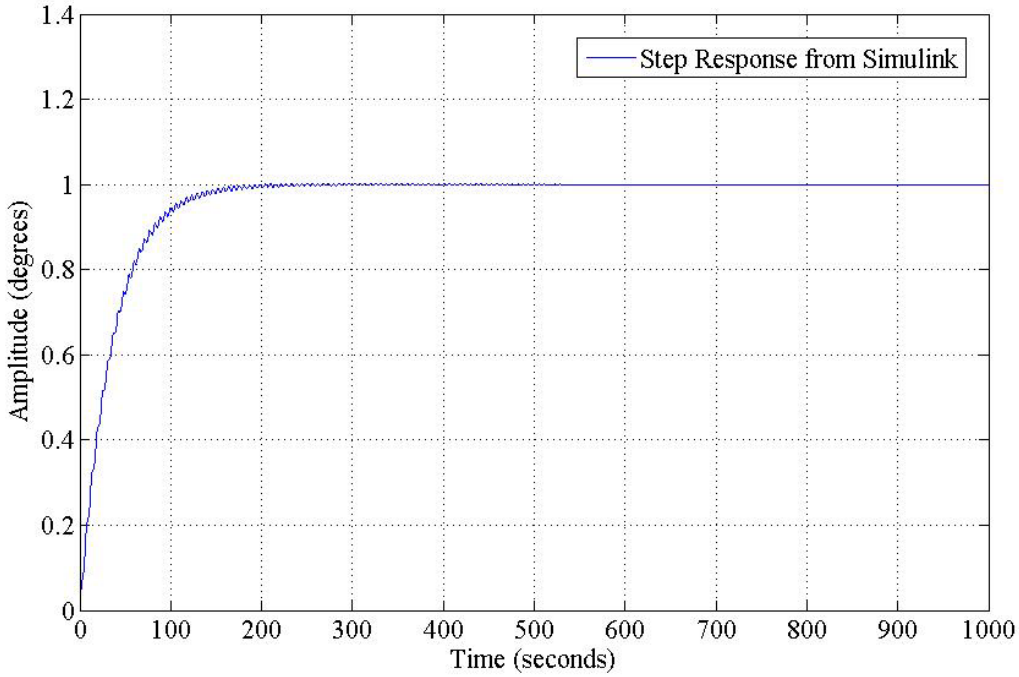

Figure 5-9: Step Response of the PDA controller simulated on Simulink.

The practical model built on Simulink obeys the theoretical model from MATLAB. Thus, we can conclude that using PDA can in fact enhance the single axis attitude control of flexible spacecraft.

Chapter 6 CONCLUSION AND FUTURE WORK

Summary: This chapter summarizes all the results obtained from this research. First we outline the theoretical accomplishments, second we conclude the results from the experiments and third we outline the results of applying our method to flexible spacecraft

6.1 Theoretical Accomplishment

We have developed a method of controlling higher order systems better by addition of acceleration feedback along with the proportional, derivative and integral feedback available in most controllers. We term it, PDA (Proportional Derivative Acceleration) control. We develop the conditions for the stability for a third order system when a PDA controller is used. We test our results with a simulated third order system on MATLAB.

We also develop a way to practically implement the controller since an acceleration sensor may not be available and the information would be derived by differentiating once or twice with an existing signal from a sensor.

We also provide a method to extend the controller design to higher order systems where the difference between the poles and zeros is either 2 or 3. We then use this control design to control a single axis attitude control of a flexible appendage. We test the controller on the parameters used for the CTS spacecraft and observed the response. We show how our control design shows a better response than the PID controller shown in References 1 and 11. We have shown also that adding acceleration feedback to the system ensured that the phase crossover frequency did not exist thus the system will not respond to flexible modes.

6.2 Experimental Accomplishment

We show how a PDA controller can be designed for a flexible link, we then demonstrate the results of the controller and compare it with the best tuned PID from Simulink. We demonstrate how we can also manually tune a PDA control by increasing proportional first, then derivative and then acceleration to control the flexible link. This proves that adding acceleration feedback helps improve the response of the system.

6.3 Limitations

The various assumptions that were made while deriving the model were presented in Sections 2.1 and 2.2. The theoretical work presented in Section 3 were built for a single input single output system in the continuous time domain. Many models in industry are multiple input multiple output systems and the code for controlling these things is in the discrete time domain. If control gains are developed using the method presented here, then the engineer must use some continuous to discrete conversions like bilinear transformation to convert the system to discrete domain. If the sensor is accepting data at a reasonably fast rate and the actuators can present output at a similarly fast rate, then the discrete time signals can be approximated to be a continuous signal.

The three axes are assumed to be uncoupled for small angle changes in the attitude control of the spacecraft, if considerable coupling is observed the control gains would have to be adjusted accordingly with the new model of the system. This should be a topic of future research.

6.4 Future Work

The next phase of research would be to test the robustness of the control design and how it

responds to disturbances. We can also expand the research to include all three axes for attitude control. Experimentally we can introduce a larger flexible link that includes many flexible modes and modify the controller if need be to try to control the system. Another approach is to study the impact of adding flexibility to a PIDA controller as in References 1 and 12.

References

1. Hughes, P. and Abdel-Rahman, T. (1979) 'Stability of Proportional-Plus-Derivative-Plus-Integral Control of Flexible Spacecraft', *Journal of Guidance, Control and Dynamics,* Vol. 2 No. 6, pp. 499-503
2. Tarek Abel-Rahman(1975) Influence of structural flexibility on a single axis attitude controller. 198, UTIAS Technical Note, Canada
3. Lafontaine, J. De. *Stability Analysis of Flexible Spacecraft with PID controller,* Communications Research Centre, Dept. of Communications, 1984.
4. Martin, Eric. DYNAMIC INTERACTION OF A SPACE MANIPULATOR WITH ITS BASE ATTITUDE CONTROLLER . 1999, www.collectionscanada.gc.ca/obj/s4/f2/dsk1/tape8/PQDD_0025/NQ50218.pdf.
5. Jung, S., & Dorf, R. (1996). Analytic PIDA controller design technique for a third order system. *Proceedings of 35th IEEE Conference on Decision and Control,* 2514-2518. Doi:10.1109/cdc.1996.573472
6. Ukakimaparn, P., Pannil, P., Boonchuay, P., & Trisuwannawat, T. (2009). 'PIDA Controller Designed by Kitti's Method' Paper presented at *ICROS-SICE International Joint Conference*
7. Dispense del Corso di (2008) Attitude Dynamics and Control. [pdf]. Retrieved from http://www.ingaero.uniroma1.it/attachments/2194_AttDyn&Control_G_Avanzini.pdf
8. Hughes, P.C., "Dynamics of Flexible Space Vehicles with Active Attitude Control," Celestial Mechanics Journal, Vol. 9, March 1974, pp. 21-39.

9. Malwatkar, G. M., Khandekar, A. A., & Nikam, S. D. (2011). PID controllers for higher order systems based on maximum sensitivity function. *2011 3rd International Conference on Electronics Computer Technology*. doi:10.1109/icectech.2011.5941601

10. Elsrogy, W. M, Fkirin, M. A, & Hassan,M. A. (2013) Speed control of DC motor using PID controller based on artificial intelligence techniques. *2013 International conference on Control, Decision and Information* Technologies (CoDIT). Doi: 10.1109/codit.2013.6689543

11. Tsuchiya, K., Inoue, M., Wakasuqi, N., & Yamaguchi, T. (1982). ADVANCED REACTION WHEEL CONTROLLER FOR ATTITUDE CONTROL OF SPACECRAVI'. *Acta Astronautica,9*(12), 697-702.

12. Froelich, R.., & Papapoff, H. (1959). Reaction wheel attitude control for space vehicles. *IRE Transactions on Automatic Control*, 4(3), 139-149. Doi: 10.1109/tac.1959.1104897

13. Skaar., S., & Kraige, L. (1982). Single-Axis Spacecraft Attitude Maneuvers Using an Optimal Reaction Wheel Power Criterion. *Journal of Guidance, Control, and Dynamics,* 5(5), 543-544. doi:10.2514/3.56200

14. Jr., R. H. (1962). Some Basic Response Relations for Reaction-Wheel Attitude Control. *ARS Journal, 32(1),* 61-74. Doi:10.2514/8.5950

15. Turner, J. D., & Junkins, J. L. (1986). Optimal Large-Angle Single-Axis Maneuvers of Flexible Spacecraft. *Optimal Spacecraft Rotational Maneuvers Studies in Astronautics,*309-357. doi:10.1016/b978-0-444-42619-2.50013-6

16. Gennaro, S. D. (2003). Passive Attitude Control of Flexible Spacecraft from

Quaternion Measurements. *Journal of Optimization Theory and Applications, 116*(1), 41-60. doi:10.1023/a:1022106118182

17. Agrawal, B., & Bang, H. (1993). Slew maneuver of a flexible spacecraft using on-off thrusters. *Guidance, Navigation and Control Conference*. doi:10.2514/6.1993-3724

18. Wie, B., & Byun, K. (1989). New generalized structural filtering concept for active vibration control synthesis. *Journal of Guidance, Control, and Dynamics,12*(2), 147-154. doi:10.2514/3.20384

19. Wie, B., Byun, K. W., Warren, V. W., Geller, D., Long, D., & Sunkel, J. (1989). New approach to attitude/momentum control for the Space Station. *Journal of Guidance, Control, and Dynamics,12*(5), 714-722. doi:10.2514/3.20466

20. Martin, Gary D, and Arthur E Bryson. (1980) "Attitude Control of a Flexible Spacecraft." Apollo 13 Guidance, Navigation, and Control Challenges | AIAA Space 2009 Conference & Exposition

21. Tieman, J., Schmalzel, J., & Krchnavek, R. (2002). Design of a MEMS-based, 3-axis accelerometer smart sensor. *2nd ISA/IEEE Sensors for Industry Conference,*19-21. doi:10.1109/sficon.2002.1159799

22. Raut, K., & Vaishnav, S. R. (2014). A Study on Performance of Different PID Tuning Techniques. Retrieved from https://www.academia.edu/4517677/A_Study_on_Performance_of_Different_PID_Tuning_Techniques?auto=download

23. Hu, Y., & Vukovich, G. (2005). Active robust shape control of flexible structures. *Mechatronics,15*(7), 807-820. doi:10.1016/j.mechatronics.2005.02.004

24. Hablani, H. B. (1992). Zero-residual-energy, single-axis slew of flexible spacecraft using thrusters - Dynamics approach. *Journal of Guidance, Control, and – Dynamics,15*(1), 104-113. doi:10.2514/3.20807

25. Han, J., Wang, Y., Tan, D., & Xu, W. (n.d.). Acceleration feedback control for direct-drive motor system. *Proceedings. 2000 IEEE/RSJ International Conference on Intelligent Robots and Systems (IROS 2000) (Cat. No.00CH37113)*. doi:10.1109/iros.2000.893161

26. Tongtanee, A., Pannil, P., Ukakimaparn, P., & Trisuwannawat, T. (2017). Discrete-time PIDA controller designed by Kittis method; a third generation. *2017 56th Annual Conference of the Society of Instrument and Control Engineers of Japan (SICE)*. doi:10.23919/sice.2017.8105730

27. Sharma, N., Bhargava, A., Sharma, A., & Sharma, H. (2016). Optimal design of PIDA controller for induction motor using Spider Monkey Optimization algorithm. *International Journal of Metaheuristics,5*(3/4), 278. doi:10.1504/ijmheur.2016.10002054

28. Auto-tuning of PID/PIDA Controllers based on Step-response. (2009). *Journal of Institute of Control, Robotics and Systems,15*(10), 974-981. doi:10.5302/j.icros.2009.15.10.974

29. Kumar, M., & Hote, Y. V. (2018). Robust CDA-PIDA Control Scheme for Load Frequency Control of Interconnected Power Systems. *IFAC-PapersOnLine,51*(4), 616-621. doi:10.1016/j.ifacol.2018.06.164

30. Chen, X., & X. (2011). Auto-Tuning Method of PIDA Controller Based Ongain Margin and Phase Margin. *International Conference on Mechanical Engineering*

*and Technology (ICMET-London 2011),*333-335. doi:10.1115/1.859896.paper65

31. Sambariya, D. K., & Paliwal, D. (2016). Optimal design of PIDA controller using harmony search algorithm for AVR power system. *2016 IEEE 6th International Conference on Power Systems (ICPS)*. doi:10.1109/icpes.2016.7584219

32. Mahmoodi, S. N., & Ahmadian, M. (2010). Modified acceleration feedback for active vibration control of aerospace structures. *Smart Materials and Structures,19*(6), 065015. doi:10.1088/0964-1726/19/6/065015

33. Fanson, J., & Caughey, T. (1987). Positive position feedback control for large space structures. *28th Structures, Structural Dynamics and Materials Conference*. doi:10.2514/6.1987-902

34. Balas, M. J. (1979). Direct Velocity Feedback Control of Large Space Structures. *Journal of Guidance, Control, and Dynamics,2*(3), 252-253. doi:10.2514/3.55869

35. Lang, Xiaoyu, et al. "Passivity-Based Attitude Control with Input Quantization." *Journal of Aerospace Engineering*, 5 Feb. 2018.

36. Hughes, Declan, and John T. Wen. "Passivity Motivated Controller Design for Flexible Structures." 1993, doi:10.21236/ada261122.

-

Appendix 1

I = 9875 kg m^2, ω_a =0.0025 rad/s, ω_s =0.5 rad/s, Z_i=0.003

Table A1 Flexible Modes of LSAT [3]

Index	Natural frequency (Ω_i)	Flexible modes constant (K_i)
1	0.999	0.000950
2	1.081	0.613892
3	1.093	0.012468
4	1.998	0.051389
5	2.256	0.000001
6	2.746	0.000004
7	3.085	0.008616
8	3.707	~0.0
9	4.229	0.000060
10	4.725	~0.0
11	5.102	0.000453
12	5.360	~0.0